INSIGHTS ON VARISCAN GEODYNAMICS FROM THE STRUCTURAL AND GEOCHEMICAL CHARACTERIZATION OF A DEVONIAN-CARBONIFEROUS GABBRO FROM THE AUSTROALPINE DOMAIN (WESTERN ALPS)

Francesco Delleani*, Gisella Rebay, Michele Zucali*,✉, Massimo Tiepolo*,° and Maria Iole Spalla***

* *Dipartimento di Scienze della Terra "A. Desio", Università degli Studi di Milano, Italy.*
** *Dipartimento di Scienze della Terra e dell'Ambiente, Università degli Studi di Pavia, Italy.*
° *C.N.R. - Istituto di Geoscienze e Georisorse UOS di Pavia, Italy.*
✉ *Corresponding author, email: michele.zucali@unimi.it*

Keywords: *Structural Map; Variscan volcanic arc; Variscan subduction; Sesia-Lanzo Zone.*

ABSTRACT

Ivozio kyanite-bearing eclogites represent one of the main pre-Alpine mafic complexes of the Sesia Lanzo Zone (Austroalpine Domain) whose protoliths have been dated at Late Devonian to Early Carboniferous. The complex consists of various HP mafic-ultramafic rocks such as amphibole-bearing eclogites, zoisite-bearing eclogites, amphibole-epidote-bearing eclogites, quartz-bearing eclogites, chlorite-bearing amphibolites and ultramafites surrounded by eclogitic micaschists and jadeite-bearing metagranitoids. Multiscale structural analyses, integrated with geochemical investigation, allowed to distinguish heterogeneities of eclogite types consequent to strain partitioning and different degrees of metamorphic re-equilibration during Alpine polyphase deformation history or to pristine magmatic differences. Five groups of Alpine structures (D_1 to D_5) have been detected: they consist of folds, foliations and shear zones developed during the Late Cretaceous to Eocene subduction-exhumation path. The metamorphic mineral assemblages related to the deformation stages indicate a polyphase deformation (pre-D_1 to D_3) under eclogite-facies conditions followed by a blueschist re-equilibration (during D_4), localized shearing and successive folding and discrete shearing (D_5) under greenschist-facies conditions. Four veining stages, developed under the eclogite- and blueschist-facies conditions have been documented.

Whole rock major and trace element composition of main igneous lithotypes suggest a subduction-related context for the emplacement of the Ivozio mafic complex. It also suggests that all rocks are not co-genetic and that they likely emplaced in the continental crust.

Igneous products with arc and back-arc geochemical affinity (from 380 to 345 Ma) are described in the European Variscan Belt from French Central Massif to Bohemian Massif, supporting the interpretation that the Ivozio mafic complex protoliths are the witness of such Devonian-Carboniferous arc magmatism in the Alpine chain.

INTRODUCTION

Metabasites enclosed in the continental crust of collisional belts are keystones to infer the ancient geodynamic settings. The pre-Alpine continental crust of Western Alps incorporates abundant mafic bodies, at present characterized by a dominant metamorphic imprint recorded under amphibolite- to eclogite-facies conditions during Alpine times (Bigi et al., 1990; Spalla et al., 2014). Their protolith ages are widespread, some of them showing Caledonian or Variscan metamorphic ages and others, more frequently, Permian-Triassic igneous ages. The Sesia-Lanzo Zone comprises several mafic bodies (Fig. 1) mostly eclogitized during Alpine subduction (e.g., Compagnoni et al., 1977; Reinsch, 1979; William and Compagnoni, 1983; Hunziker et al., 1992; Venturini, 1995; Rebay and Messiga, 2007; Gosso et al., 2010; Spalla et al., 2010; Rebay et al., 2015). In spite of their penetrative Alpine structural and metamorphic re-equilibration, numerous relics indicate that pre-Alpine protoliths were gabbros, granulitized gabbros (mainly with Permian age) and granulites (variably re-equilibrated under amphibolite- and greenschists-facies conditions), amphibolites and hornblendites (e.g., Bianchi et al., 1965; Viterbo-Bassani and Blackburn, 1968; Compagnoni et al., 1977; Lardeaux et al., 1982; Lardeaux and Spalla, 1991; Venturini et al., 1991; Venturini et al., 1996; Bussy et al., 1998; Rebay and Spalla, 2001; Gosso et al., 2010).

In the internal part of the Sesia-Lanzo Zone (Eclogitic Micaschist Complex) most of metabasites have been fully transformed into eclogites and glaucophanites during Alpine subduction. Protoliths of these metabasic rocks may be of various origin, as pre-Alpine eclogites, basaltic dykes or gabbros, Permian or even older. This is the case of eclogites of the Ivozio mafic complex, comprising metre-thick ultramafic layers, with magmatic ages of 355±9 Ma (Rubatto, 1998). The Ivozio mafic complex are described as Fe-gabbros, genetically related to other MORB gabbroic intrusions, further suggesting an oceanic pertinence of the protoliths (Pognante et al., 1980; Venturini et al., 1991; Venturini 1995; Rubatto, 1998; Rubatto et al., 1999; Zucali et al., 2004; Delleani et al., 2011; Delleani et al., 2012b). The gabbroic Complex, including various type of eclogitic metabasites and scarce ultramafites, locally preserves the primary magmatic layering (Pognante et al., 1980; Zucali et al., 2004; Delleani, 2013) and is therefore an interesting subject of structural investigation for deciphering pre-Alpine textural and compositional characters, fundamental to shed light on the geodynamic environment in which this gabbroic complex was emplaced.

This contribution aims at illustrating variations of bulk rock compositions across this Carboniferous gabbroic complex. Studied samples have been selected after a detailed multiscale structural and petrographic analysis devoted at individuating the domains less affected by the Alpine imprint. To this purpose, the analytical data are illustrated with the support of a petro-structural map (Fig. MAP), on which highly deformed domains, referred to successive Alpine deformation stages, are contoured.

GEOLOGICAL SETTING

The gabbroic Complex (Pognante et al., 1980; Zucali et al., 2004; Zucali and Spalla, 2011) is part of the Eclogitic Micaschist Complex of the Sesia-Lanzo Zone. The Sesia-Lanzo Zone (SLZ) (Fig. 1) consists of four complexes (Roda et al., 2012; Cantù et al., 2016): 1) Seconda Zona Diorito-Kinzigitica (IIDK); 2) Eclogitic Micaschist Complex (EMC); 3) Gneiss Minuti Complex (GMC) and 4) Rocca Canavese Thrust Sheet (RCTS).

The Seconda Zona Diorito-Kinzigitica (IIDK) consists of km-sized lenses of high-grade continental crust (i.e. diorite-kinzigite) that largely escaped the Alpine eclogitic re-equilibration. The Eclogitic Micaschist Complex (EMC) pervasively records the eclogitic phase and only locally the greenschist one, whereas the Gneiss Minuti Complex (GMC) is mostly recording the post-eclogitic greenschist facies mostly associated to mylonitic textures (Spalla et al., 1983; Stuenitz, 1989; Spalla et al., 1991; Wheeler and Butler, 1993; Babist et al., 2006). The EMC constitutes the innermost part of the SLZ, where the exhumation-related greenschist imprint is confined to discrete shear zones (e.g., Zucali et al., 2002; Babist et al., 2006) and is more pervasive toward the inner boundary with the Southern Alps, marked by the Periadriatic Lineament. The Rocca Canavese Thrust Sheet (RCT) consists of thin crustal slices located along the eastern margin of the southern SLZ and extends from Rocca Canavese to Courgnè, (Fig. 1b; Pognante, 1989a; 1989b). It consists of pre-Alpine granulites, serpentinized tectonitic lherzolites, glaucophane-bearing schists and metagranitoids. The eclogite-facies conditions affecting the EMC (Fig. 1c) and the GMC are not described in the RCT. Based exclusively on the inferred metamorphic evolutions, the coupling between the IIDK, EMC, GMC and RCT has been interpreted to occur under blueschist facies conditions, synchronous with the early exhumation stages of the EMC (Pognante, 1989a; Spalla and Zulbati, 2003; Cantù et al., 2016).

P-T estimates for the pre-Alpine evolution of the SLZ show a granulite facies imprint in a pressure interval between 0.6-0.9 GPa at T = 700-900°C, followed by an amphibolite facies imprint defined by P = 0.3-0.5 GPa and T = 570-670°C and a greenschist facies re-equilibration at P = 0.25-0.35 GPa and T < 550°C (Lardeaux and Spalla, 1991; Rebay and Spalla, 2001). Geo-chronological determinations and field relationships attribute an age of ≤ 270 Ma to the granulite facies stage, an age of ≈ 240 Ma to the amphibolite facies, and an age of ≈ 170 Ma to the greenschist facies metamorphism. The Alpine eclogite-facies evolution (Koons, 1982; Castelli, 1991; Tropper et al., 1999; Tropper and Essene, 2002; Zucali et al., 2002; Zucali and Spalla, 2011) mainly ranges between 60 and 80 Ma with several older ages (e.g., Hunziker, 1974; Oberhaensli et al., 1985; Stoeckhert et al., 1986; Hunziker et al., 1992; Reddy et al., 1996; Rubatto, 1998; Rubatto et al., 1999; Handy and Oberhaensli, 2004; Cenki-Tok et al., 2011; Rubatto et al., 2011; Zucali and Spalla, 2011; Regis et al., 2014) at P = 1.6-2.4 GPa and T = 500-550°C.

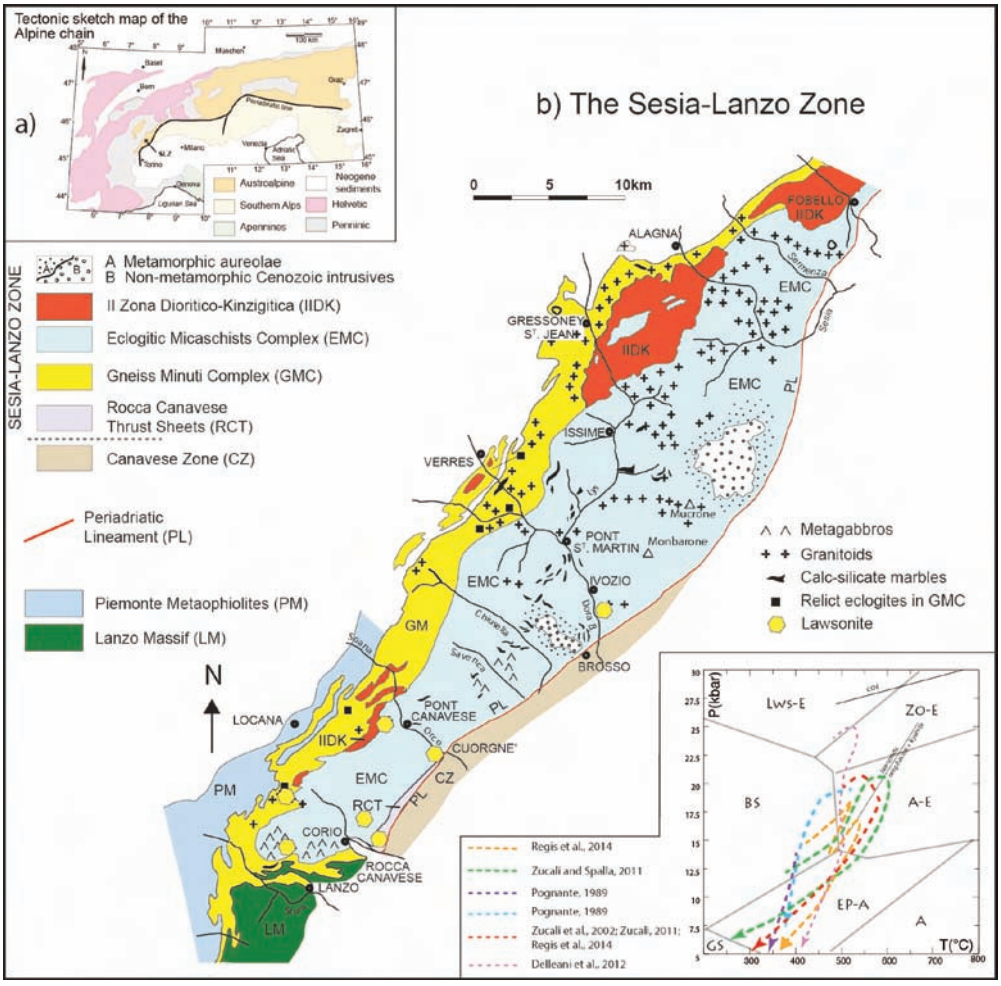

Fig. 1 - a) Sketch of the Alpine chain; b) the Sesia-Lanzo Zone and its subdivision into main complexes and units. c) Alpine P-T paths of the Eclogitic Micaschist Complex.

The gabbroic Complex consists of a wide variety of eclogitic metabasites (including lawsonite-kyanite eclogites) and scarce ultramafics (metapyroxenites and antigorite-serpentinites); primary magmatic layering has also been observed (Pognante et al., 1980; Zucali et al., 2004; Zucali and Spalla, 2011) with magmatic ages of 355±9 Ma (Rubatto, 1998). These rocks have been folded during eclogite to blueschists facies conditions, while greenschist facies deformation refolds the main contact between the Ivozio mafic complex and the surrounding paraschists and metagranitoids of the EMC (Pognante et al., 1980; Zucali et al., 2004; Delleani, 2013).

The particularly high Pressure-Temperature ratio characterizing the Alpine evolution of the SLZ continental crust enhanced the preservation in Alpine low-strain domains of relic pre-Alpine assemblages, from granulite to greenschist facies conditions (Dal Piaz et al., 1971; 1972; Compagnoni et al., 1977; Gosso, 1977; Lardeaux, 1981; Spalla et al., 1983; Williams and Compagnoni, 1983; Lardeaux and Spalla, 1991; Rebay and Spalla, 2001; Zucali, 2011; Delleani et al., 2012a; 2012b; Corti et al., 2017 and references therein). In analogy to the evolutions recorded in other portions of the Austroalpine and Southalpine continental crust (e.g., Diella et al., 1992; Bertotti et al., 1993; Dal Piaz, 1993; Bertotti and der Voorde, 1994; Handy et al., 1999; Schuster et al., 2001; Schuster and Stuewe, 2008; Marotta et al., 2009; Manzotti and Zucali, 2013; Spalla et al., 2014), the granulite to amphibolite pre-Alpine PT evolution has been interpreted as representative of an extension-related uplift during Permian-Triassic times (e.g., Lardeaux and Spalla, 1991; Rebay and Spalla, 2001; Spalla and Marotta, 2007; Marotta et al., 2016).

LITHOSTRATIGRAPHY OF THE EMC

Micaschists are fine-grained rocks containing white mica, quartz, blue-green amphibole, Na-clinopyroxene, garnet and zoisite. Grey white mica with a grain-size up to 5mm, marks the mm-thick continuous foliation wrapping elongated and flattened lenses of microcrystalline quartz. Microlithons frequently contain a relic foliation, mainly marked by isoriented white mica crystals. Fine-grained amphiboles vary from dark-blue (Ca-Na amphibole) to pale violet (glaucophane) in colour and clinopyroxenes from pale- to dark-green (omphacite or jadeite); pinkish garnets and zoisite are very fine-grained. Mineral modal amount in micaschists is heterogeneous: quartz varies from 15% to 40%, white mica from 20% to 40%, and amphibole from 5% to 20%. Locally, micaschists contain fine-grained white albite, greenish chlorite and yellowish epidote mainly replacing white mica, clinopyroxene and garnet. Rutile, titanite and apatite may occur as accessory minerals.

Metagranitoids occur in layers from 1- to 10-metres-thick (Fig. 2a). They are medium to coarse-grained rocks composed of quartz, white mica, jadeite and K-feldspar porphyroclasts. Medium to coarse-grained quartz generally forms lenses and layers up to 3 cm thick, white mica is pale-green and jadeite is pale-green or whitish. It may occur in porphyroblasts, up to 8 cm in size containing abundant quartz and white mica inclusions. White mica and jadeite SPO underline a discontinuous foliation in which lenticular quartz-domains are elongated. Locally, fine-grained white albite and yellowish Fe-epidote develop at the expenses of jadeite and white mica. Glaucophane, garnet, rutile, titanite and chlorite can be accessory minerals.

The protoliths of the Ivozio mafic complex consists of rocks with different igneous compositions, now detectable as layers with different mineral assemblages. They are characterized by decimetre to ten-metres thickness. This primary lithologic layering is well detectable only in domains that escaped the strong Alpine deformation. On the contrary, in high-strain domains the primary magmatic layering is frequently obliterated and the mineral assemblages testify the strong interaction between deformation and metamorphism. Using petro-structural analysis, six lithotypes have been distinguished: *amphibole-bearing eclogites*; *zoisite-bearing eclogites*; *amphibole-epidote-bearing eclogites*; *quartz-bearing eclogite*; *chlorite-bearing amphibolites*; *ultramafites*.

Amphibole-bearing eclogites have ≥ 30% (volume) of blue-green amphibole and are medium- to fine-grained rocks, containing also garnet, omphacite, white mica and zoisite. Accessory minerals are generally chlorite, epidote, rutile, titanite, quartz and albite. Rare relic prismatic domains formed by zoisite and paragonite aggregates are interpreted as pseudomorphs on lawsonite. In this eclogite type amphibole-, garnet- and omphacite-rich layers frequently alternate (Fig. 2b and c). This layering has been transposed parallel to D_1 axial planes and has been mapped as S_1 within amphibole-bearing eclogites. The boundary between juxtaposed layers can be transitional or discrete (Fig. 2c) and locally is marked by mm-thick epidote-rich layers. The gradual transition between amphibole- and garnet-rich layers can result from the metamorphic transformation of a poorly deformed original igneous layering. At the meso-scale these alternating layers do not show mineral SPO.

Amphibole-rich layers are composed of medium- to fine-grained blue/blue-green amphibole (50-70%), garnet (15-30%) and omphacite (10-30%). Amphibole has blue rims around blue-green coloured cores and is fine-grained. Garnet is pinkish, and fine-grained with rare poikiloblasts of cm-size. Green omphacite occurs in medium-grained crystals, up to cm-long, and as fine-grained, 1 to 3mm long needles.

Garnet rich layers contain medium- to fine-grained garnet (60-80%), blue-green amphibole (40-20%) and omphacite (5%). Garnet is pinkish, medium-grained, and locally in poikiloblasts. Amphibole is blue-green and fine-grained; rare acicular omphacite is fine-grained.

Omphacite-rich layers generally lie between amphibole- and garnet-rich layers. These layers are composed of medium- to coarse-grained omphacite (40-60%), amphibole (20-30%), white mica (15-25%) and garnet (5%). Omphacite is coarse-grained, up to cm-size, with emerald green colour. Amphibole is fine-grained, with blue-green colour, and occupies the interstices between omphacite and white mica. White mica is medium- to coarse-grained, up to cm-size, and is pale-grey with silky sheen. Rare pinkish, fine-grained, garnet crystals occur. Omphacite and white mica crystals are randomly oriented in these layers.

Zoisite-bearing eclogites contain at least 30 vol% of white zoisite. They are medium- to coarse-grained rocks constituted by zoisite (30-60 vol%), blue amphibole (15-35 vol%), white mica (15-25 vol%), garnet (10-20 vol%), omphacite (10-20 vol%) and quartz (5-15 vol%). Zoisite is medium- to coarse-grained, up to cm-size and tabular-shaped. Blue amphibole is fine- to medium- grained. White

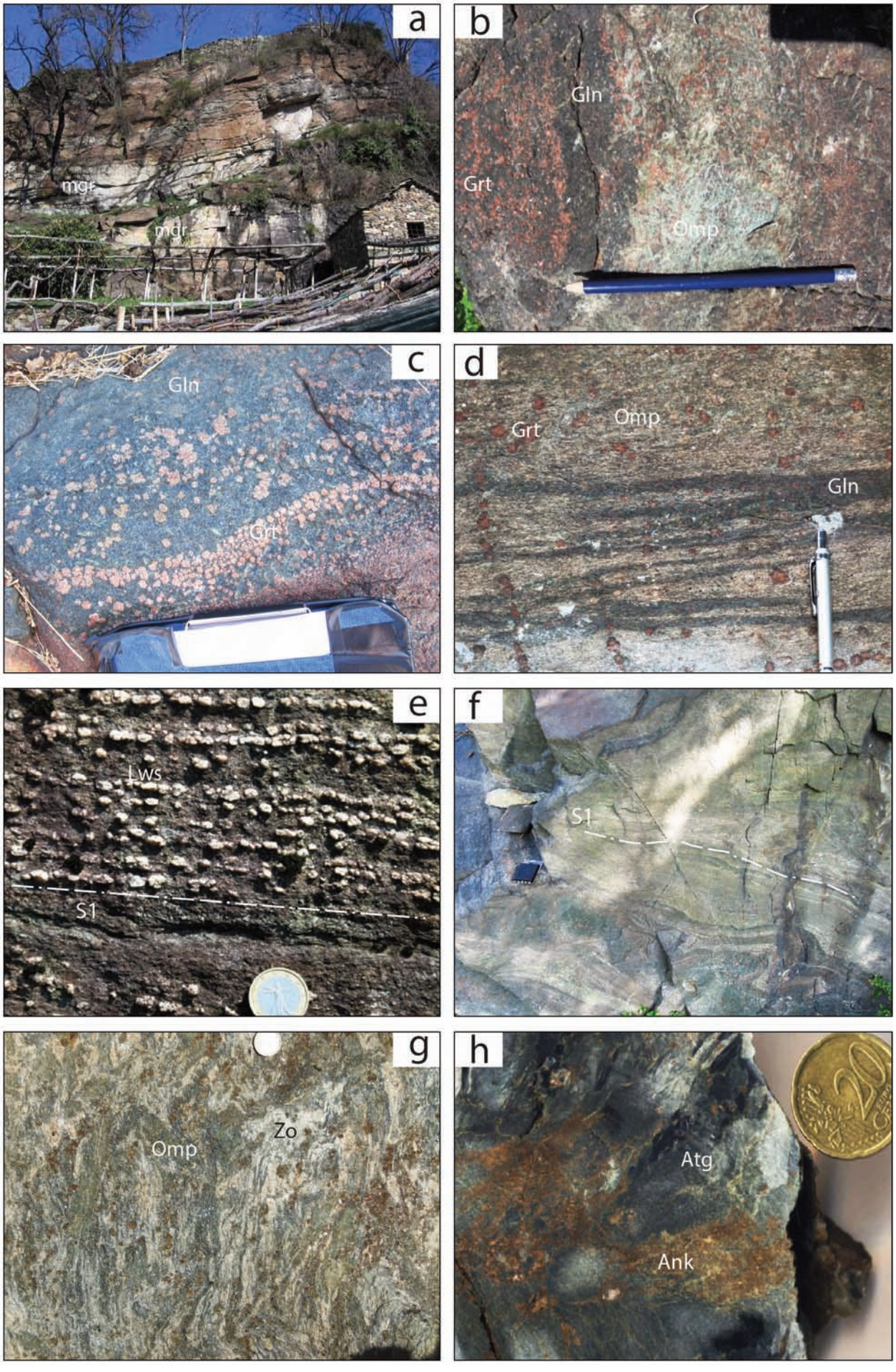
a
mgr
mdr
b
Gln
Grt
Omp
c
Gln
Grt
d
Grt
Omp
Gln
e
Lws
S1
f
S1
g
Omp
Zo
h
Atg
Ank

mica is medium-grained, pale-grey phengite and silver white paragonite. Garnet is reddish and medium- to coarse-grained, with up to cm-grain size (Fig. 2d). Coarse-grained emerald green crystals of omphacite are up to 5 cm in length. Quartz is fine-grained and occurs within mm- to cm-thick lenses. Locally these rocks contain up to 10 cm porphyblasts of garnet and up to 35% of white mica. Chlorite, epidote, rutile, titanite and albite are accessory minerals. These eclogites generally preserve textural relics of lawsonite (Fig. 2e), as prismatic coarse-grained domains, up to 3 cm in length, pseudomorphosed by whitish aggregates of zoisite + paragonite. Locally these domains are bluish and made by kyanite, testifying the replacement of lawsonite, as described by Zucali et al (2004) and Zucali and Spalla (2011). Coarse-grained zoisite, white mica and blue-amphibole show SPO parallel to S_1; also, lawsonite pseudomorphs are aligned within S_1. In places, S_2 marked by fine-grained omphacite, white mica and zoisite wraps around pseudomorphosed lawsonite porphyroblasts and around omphacite and garnet large-sized porphyroblasts (3-10 cm).

Amphibole-epidote-bearing eclogites are banded rocks with 5- to 15-cm thick alternating layers rich in dark-green amphibole or epidote (Fig. 2f). This layering has been transposed parallel to D_1 axial planes and has been mapped as S_1, as in amphibole-bearing eclogite. Dark-green amphibole, omphacite and garnet trails mark S_2 foliation in D_2 high strain domains.

Amphibole-rich layers contain medium- to fine-grained dark-green amphibole (70-90 vol%), garnet (10-20 vol%) and omphacite (5-15 vol%). Garnet is pinkish and medium- to coarse-grained (up to 2cm) and omphacite is green and medium-grained. White mica, chlorite, epidote, rutile, titanite, quartz and albite are accessory minerals.

Epidote-rich layers contain fine-grained epidote (60-70 vol%), dark-green amphibole (20-30 vol%) and chlorite (5-10 vol%). Epidote is yellow-green and fine-grained, dark-green amphibole is fine-grained, and chlorite is greenish and very fine-grained. Omphacite, garnet, white mica, rutile, titanite, quartz and albite are accessory phases. Omphacite is randomly oriented as in the other eclogite types.

Quartz-bearing eclogites have ≥ 30 vol% quartz. They contain zoisite (30-50 vol%), quartz (30-50 vol%), omphacite (20-40 vol%) and white mica (5-15 vol%), and are coarse-grained. Zoisite occurs in coarse-grained (up to 3cm) prismatic white crystals, quartz is medium- to fine-grained and occurs within cm-thick lenses, omphacite is emerald green and coarse-grained (locally up to 5cm in length), and white mica is pale-grey. Blue amphibole, garnet, chlorite, epidote, rutile, titanite and albite are accessory phases. Quartz-bearing eclogites mainly show a 5-cm-spaced discontinuous S_1 foliation marked by SPO of coarse-grained zoisite and white mica, and by lenticular quartz domains. Minor volumes record cm-spaced discontinuous S_2 foliation marked by medium- to fine-grained zoisite and white mica wrapping around large omphacite porphyroblasts (3-5cm) and quartz elongated lenses (Fig. 2g).

Chlorite-bearing amphibolites are medium- to fine-grained amphibole-bearing rocks constituted by amphibole (50-70 vol%), chlorite (20-30 vol%), epidote (10- 20 vol%.), white mica (5-10 vol%) and omphacite (5-10 vol%). Amphiboles are medium-grained crystals, chlorite is pale-green and fine-grained, epidote has green yellowish colour and is medium- to fine-grained, and emerald green omphacite is medium- to coarse-grained. K-feldspar, quartz and albite are accessory minerals. These rocks mainly record cm-spaced S_2 foliation marked by green-amphibole, omphacite, chlorite, epidote and white mica SPO.

Ultramafites are antigorite-serpentinites and meta-pyroxenites constituting 1 to 5 m-thick layers within eclogites.

Antigorite-serpentinites (Fig. 2h) contain fine-grained dark-green antigorite (60-70 vol%), chrysotile (10-20 vol%), carbonates (10-20 vol%.) and magnetite (5-10 vol%.). White fibrous chrysotile fills fractures of the antigorite-serpentinites. Carbonates are red-coloured and fine-grained and are preserved in cm-sized domains. Magnetite is very fine-grained (< 1mm). Tremolite, Mg-chlorite and diopside are accessory phases. Antigorite-serpentinites always show a mm-thick dominant foliation marked by medium-grained antigorite, chlorite and minor tremolite.

Meta-pyroxenites comprise diopside (40-60%), tremolite (20-30%), omphacite (10-20%) and Mg-chlorite (10-20%). Diopside and tremolite have a similar bright green colour, they form medium- to coarse-grained porphyroclasts, omphacite is emerald green and medium-grained, and Mg-chlorite is colourless and fine-grained. White mica, and zoisite may occur as accessory minerals. Meta-pyroxenites record a 10-cm-spaced S_2 foliation marked by fine-grained Mg-chlorite, tremolite and diopside, wrapping medium-grained tremolite and diopside crystals. Medium-grained omphacite is randomly oriented as in the other lithotypes.

DEFORMATION HISTORY

A detailed mapping, performed integrating structural and petrographic analysis at different scales (Gosso et al., 2015 and refs. therein) allowed to recognize five groups of Alpine superposed structures (D_1 to D_5).

They consist of fold systems, foliations and shear zones developed during the Alpine subduction-exhumation cycle, with the metamorphic mineral assemblages related to the deformation stages indicating eclogite- to greenschist-facies conditions. Moreover, four veining stages, developed under eclogite- and blueschist-facies conditions.

Fig. 2 - Mesoscopic characters of Ivozio mafic complex lithotypes and surrounding rocks. Mineral abbreviations according to Whitney and Evans. (2010), Wm = white mica. a) Metre-thick layers of leucocratic metagranitoids (mgr in Fig. 2a) intercalated in the eclogitized micaschists surrounding the Ivozio mafic complex; b) alternating amphibole-, garnet- and omphacite-rich layers with cm-thickness in amphibole-bearing eclogite; c) gradual transition between amphibole- and garnet-rich layers in amphibole-bearing eclogite, evidenced by progressive impoverishment of fine-to medium grained garnet trails; d) reddish coarse-grained garnet porphyroblasts in zoisite-bearing eclogite; e) medium-grained textural relics of lawsonite in trails in zoisite-bearing eclogite; f) amphibole and epidote 10-cm-thick layers of the amphibole-epidote-bearing eclogite parallel to S_1 foliation bent by D_2 folds; g) S_2 mm-thick foliation in quartz-bearing eclogite marked by fine-grained zoisite, white mica and omphacite, with large cm-thick syn/post-$_D$ omphacite crystals crenulated during D_3; h) antigorite-serpentinite with mm-spaced foliation, which wraps around ankerite aggregates. Thin fractures filled by fibrous chrysotile crosscut both foliation and ankerite aggregates.

Table 1 - Deformation/metamorphism relationships in the Ivozio mafic complex lithotypes.

	D1	post-D1	D2	D3	D4	D5
Amphibole-bearing eclogite	Ed, Grt, Wm and Zo	Lws / Ky (late)	Na-Amp, Zo, Grt, Omp, Ky(early), Ph and Pg /late)	Qz, Na-Amp/Ed, Ph, Pg and Czo	Gln, Ph, Mg-Chl, Di and Czo	Wm, Ab, Ep, Fe-Chl and Ed
Zoisite-bearing eclogite	Qz, Zo, Ed/Act, Wm and Grt	Lws / Ky (late)	Qz, Omp, Na-Ca Amp, Grt, Zo, Ky (early), Pg(late), Mg Chl and Ph	Qz, Ca-Na Amp/Ed, Ph, Pg and Czo	/	Wm, Ab, Ep, Fe-Chl and Ed
Amphibole-epidote bearing eclogite	Ed, Ep, Mg-Chl and Wm (pre-D2)	/	Prg, Wm, Mg-Chl, Grt, Di and Czo	/	/	Wm, Ab, Ep, Fe-Chl and Ed
Quartz-rich eclogite	Qz, Zo, Amp, Wm and Grt	/	Qz, Omp, Amp, Grt, Zo, Ph and Pg (late)	Qz, Amp, Ph, Pg and Czo	/	Wm, Ab, Ep, Fe-Chl and Ed
Chlorite-amphibolite	Ath and Wm (pre-D2)	/	Na-Amp, Ph and Mg Chl	/	/	Wm, Ab, Ep, Fe-Chl and Ed
Antigorite serpentinite	Ol (pre-D2)	/	Atg, Ged, Mg-Chl and Cb(Atg foliation)	/	/	Ctl, Mg-Chl and Cb
Metapyroxenite	Di, Tr/Act and Mg-Chl (pre-D2)	/	Di, Tr/Act/Ed, Mg-Chl, Phl and Ph	/	/	Wm, Ab, Ep, Fe-Chl, Ed/Act

Relationships between the superposed fabrics and successive mineral assemblages allowed to infer the following metamorphic and structural evolution (Table 1 and Fig. 3):

- pre-D_1 stage (intrusive layering)
- D_1 stage (folding and S_1 foliation)
- D_1 stage (garnet-bearing veining)
- D_2 stage (folding and S_2 foliation)
- D_2 stage (omphacite- and garnet-bearing veining)
- D_3 stage (folding and S_3 foliation)
- D_4 stage (localized shearing)
- D_4 stage (glaucophane- and zoisite-bearing veining)
- D_5 stage (folding and shearing)

Pre-D_1 stage (intrusive layering)

Transitional contacts between layers defined by varying modal compositions related to the pre-Alpine igneous layering are still preserved in some poorly deformed volumes of the amphibole-bearing eclogites and amphibole-epidote-bearing eclogites. They are represented by amphibole and garnet layers in amphibole-bearing eclogites and by amphibole and epidote layers in amphibole-epidote-bearing eclogites, respectively (Fig. 2b, c and d).

D_1 stage (folding and S_1 foliation)

D_1 stage produced to 0.1 to 1 m-sized folds, rarely visible in the field (Fig. 3a). In zoisite-bearing eclogites and quarz-rich eclogites the S_1 foliation is marked by isoriented blue-amphibole, white mica and zoisite, usually oriented parallel to the lithological banding (Fig. MAP and Fig. 4). Locally, in amphibole- and amphibole-epidote-bearing eclogites the S_1 foliation is preserved in garnet trails while in meta-pyroxenites no S_1 occurs. In ultramafites the S_1 foliation is marked by medium-grained antigorite, Mg-chlorite and tremolite. S_1 poles show a girdle distribution along NNW-SSE direction with a stronger distribution for west dipping planes with dipping angles < 30° (Fig. 4).

D_1 stage (garnet-bearing veining)

Garnet-bearing veins, composed of pinkish medium-grained garnet trails (Fig. 3b), are common in amphibole-, amphibole-epidote- and zoisite-bearing eclogites. In amphibole-bearing eclogites, they are localized in amphibole layers as 10- to 30-cm long garnet trails oriented at a high angle to the layering (Fig. 3f). In syn-D_2 high-strain domains, garnet-bearing veins always crosscut the S_1 foliation and are transposed parallel to the S_2 foliation. In zoisite-bearing eclogites, garnet-bearing veins have a lateral continuity of up to 2 m with garnet up to 2 cm-size.

D_2 stage (folding and S_2 foliation)

1 m to 10 m folds (Fig. 3b), with wavelengths of 2 to 10 m, characterize the D_2 stage. D2 folds deform the contact between the Ivozio mafic complex and the surrounding EMC. In amphibole-bearing eclogites, the S_2 fine-grained

Fig. 3 - Mesostructural characters of Ivozio mafic complex. a) D_1 folding of garnet- and amphibole-rich alternating layers in amphibole-bearing eclogite. White dotted and dashed line is the axial surface trace of D_1 fold; b) similar-shaped syn-D_2 fold marked by a 10 cm-thick amphibole-rich layer within a zoisite-bearing eclogite; c) D_3 fold bending S_2 foliation in a zoisite-bearing eclogite; d) S_4 continuous mylonitic foliation in a 2 m-thick glaucophane-bearing shear zone developed in amphibole-bearing eclogite; e) 3 cm-thick syn-D_5 shear zone marked by fine-grained chlorite in amphibole-epidote-bearing eclogite; f) garnet-bearing veins cutting amphibole- and garnet-rich alternating layers, parallel to S_1, in amphibole-bearing eclogite. These veins are deformed during D_2; g) omphacite-bearing veins at a high angle with S_2. These veins are up to 10 cm-thick; h) glaucophane-bearing veins, containing minor zoisite (creamy colour) in amphibole-bearing eclogite; these veins develop during D_4.

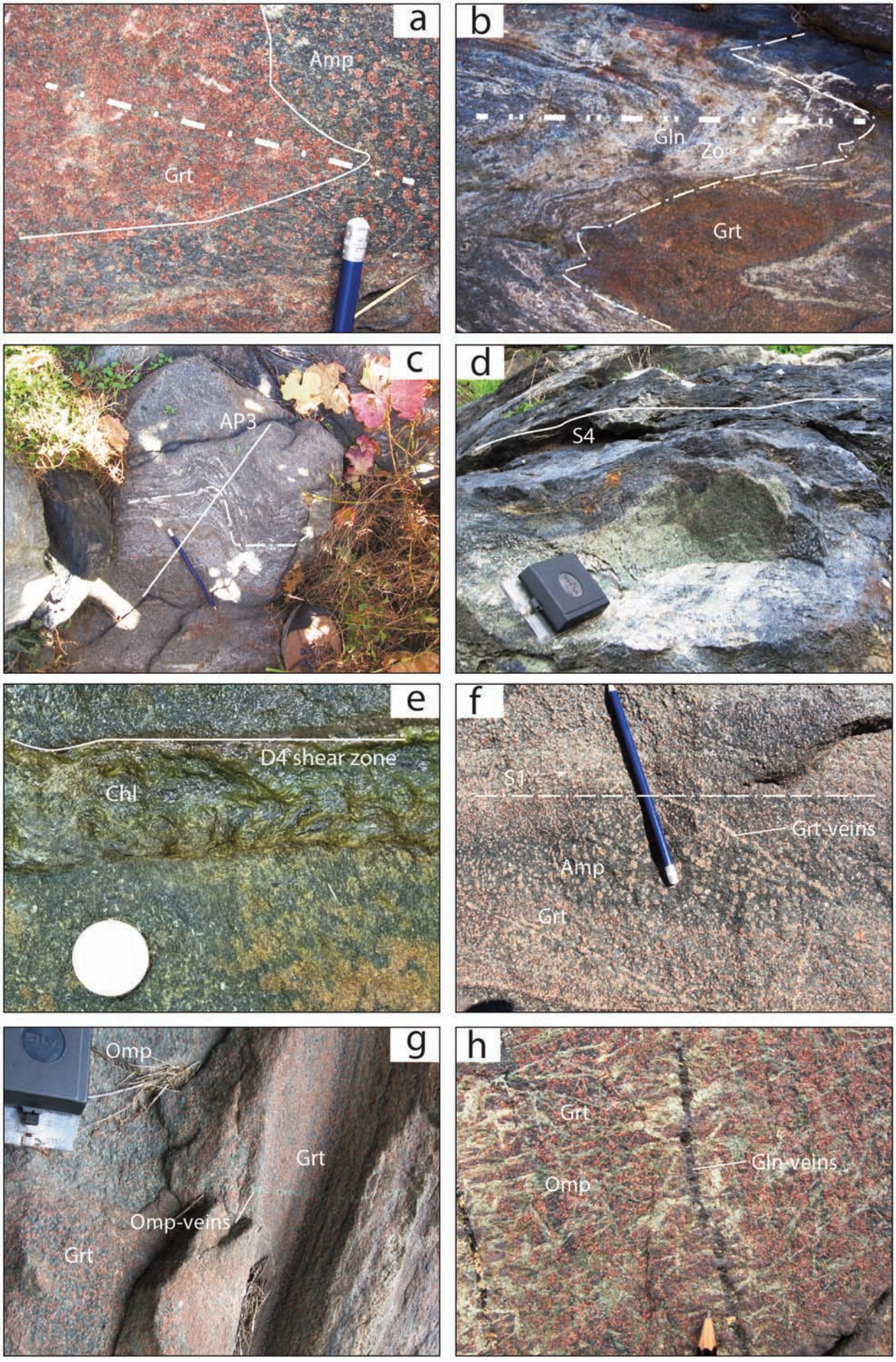
a
Amp
Grt
b
Gln
Zo
Grt
c
AP3
d
S4
e
D4 shear zone
Chl
f
S1
Grt-veins
Amp
Grt
g
Omp
Grt
Omp-veins
Grt
h
Grt
Gln-veins
Omp

mm-spaced foliation is localized in 10 to 20 m thick bands. It is marked by isoriented omphacite that replaces syn-D_1 amphibole. In poorly-foliated amphibole-bearing eclogites the main effect of syn-D_2 transformations is the development of poorly to randomly oriented medium- to coarse-grained omphacite crystals. In zoisite-bearing eclogites and quartz-bearing eclogites, S_2 is a cm-spaced foliation marked by the SPO of medium-grained omphacite, blue-amphibole, white mica and zoisite (Fig. 3c). Around omphacite and garnet coarse-grained porphyroclasts, S_2 shows a mylonitic fabric with mm spacing and very small grain size. In zoisite-bearing eclogites the S_2 foliation always wraps lawsonite pseudomorphs. In metapyroxenites, fine-grained diopside, tremolite and Mg-chlorite mark the S_2 foliation. S_2 foliation is sub-horizontal (Fig. 4), mainly dipping toward south. Syn-D_2 axial planes show a similar orientation, having low dipping angles and dip directions at SW. The D_2 axes are dispersed with the axial planes, probably accounting for a non-cylindrical shape of D_2 folds (Fig. 4 and Fig. MAP).

D_2 stage (omphacite- and garnet-bearing veining)

Omphacite- and garnet-bearing veins are rare and crosscut the S_1 and S_2 foliations. In zoisite- and amphibole-bearing eclogites, omphacite/garnet, quartz, and phengite (Fig. 3g) fill 1 to 10 cm -thick fractures. Their lateral continuity is 10m maximum. Omphacite overgrows mineral assemblages of the enclosing rocks at the margins of the veins.

D_3 stage (folding and S_3 foliation)

D_3 stage produced close to open folds with 1 to 10 m wavelength and a S_3 axial plane foliation marked by fine-grained blue amphibole, zoisite and white mica. They were documented in all lithotypes. It is associated to fine-grained S_3 foliation marked by blue amphibole, zoisite and white mica. D_3 folds have sub-vertical axial planes striking N-S (Fig. 3c and Fig. MAP).

D_4 stage (localized shearing)

D_4 stage produced a set of sub-horizontal shear zones. They occur within amphibole-bearing eclogites (Fig. 3d). The S_4 mm-spaced foliation is marked by abundant glaucophane with minor epidote and white mica and displays a mylonitic fabric.

D_4 stage (glaucophane- and zoisite-bearing veining)

Glaucophane-bearing veins occur in all lithotypes, with the exception of ultramafics. These veins have a lateral continuity of 10 to 20 m and are further evidenced by the growth of fine-grained glaucophane halos in the country rocks (Fig. 3h and Fig. MAP). Rare zoisite-bearing veins almost parallel to the glaucophane-bearing veins occur in amphibole- and zoisite-bearing eclogites; they are fractures, up to 1 cm wide, filled by fine-grained syntactical growth of zoisite, and have a lateral continuity of maximum 2 m. Glaucophane- and zoisite-bearing veins crosscut D_3 structure and they are lately deformed by D_5 fold system.

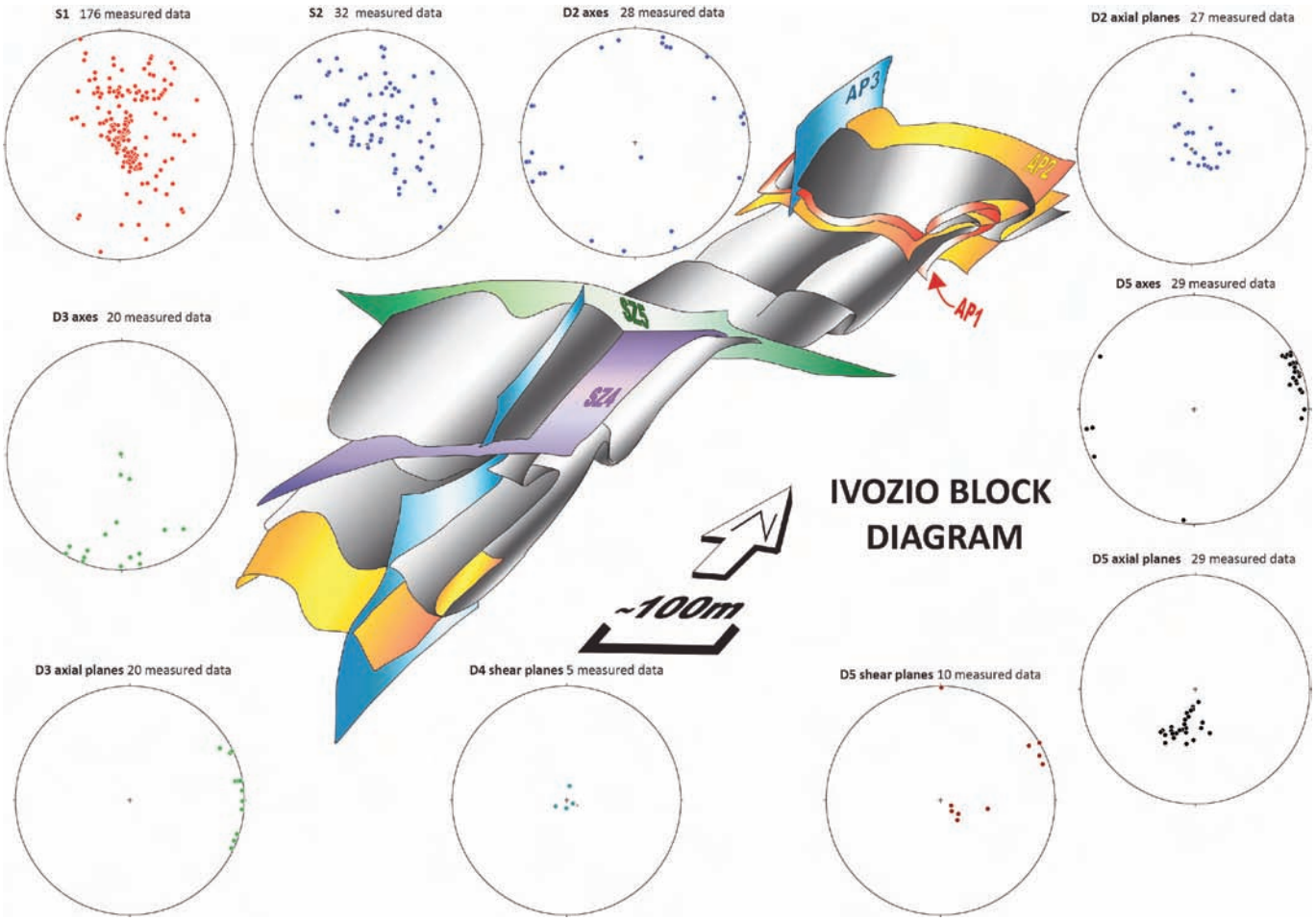

Fig. 4 - Schematic block diagram showing the Ivozio mafic complex structural setting resulting from overprinting of D_1, D_2, D_3 and D_5 folding and from D_4 and D_5 shear zones. Stereographic projections of D_1-D_5 structural elements are also shown.

D_5 stage (folding and shearing)

D_5 stage produced gentle to close folds (Fig. MAP), occurring in all the lithotypes and folding all pre-existing structural features. In poorly deformed domains, fine-grained albite, chlorite, green amphibole, white mica and epidote overgrow previous minerals, especially substituting omphacite and garnet. D_5 axial planes, NNE dipping with angles between 20 and 50°, have sub-horizontal axes oriented at about 80°N (Fig. MAP). D_5 is associated to cm- to m-thick shear zones (Fig. 3e) and the mm-sized S_5 mylonitic foliation is marked by SPO of fine-grained chlorite, green amphibole, albite, white mica and epidote.

The overprinting relationships between D_1, D_2, D_3 and D_5 folding and D_4 and D_5 shear zones are synthesized in the block diagram of Fig. 4. Alpine veining is polyphase (post-D_1 and syn-D_4) and may be related to the de-hydration reactions of Lws and Amp (post-D_1), substituted respectively by kyanite and omphacitic pyroxene. Syn-D_4 veins are localized near and within D_4 shear zones and develop during hydration associated with P and T retrograde path and are characterized by the occurrence of new hydrated phases such as amphibole and epidote suggesting an incoming fluid phase within the system.

MICROSTRUCTURE AND METAMORPHIC EVOLUTION

In the following section the microstructural features documented in different lithotypes are described separately and a summary is given in Table 1.

Amphibole-bearing eclogite

D_1 relics are represented by rare blue-green amphibole porphyroclasts, reddish cores of garnet crystals (and their inclusions of blue-green amphibole, epidote, magnetite and rutile), and inclusions of syn-D_1 blue-green amphibole and phengite preserved in large syn-D_2 omphacite crystals. In high-strain D_2 domains, the mm-sized S_2 foliation is principally marked by isoriented fine-grained omphacite, phengite, zoisite and glaucophane (Fig. 5a). In low-strain D_2 domains, pinkish garnet develops as new crystal or as rims around syn-D_1 garnet, atoll-shaped; glaucophane partially replaces syn-D_1 blue-green amphibole; omphacite and phengite occur as randomly oriented medium- to coarse-grained crystals. Coarse-grained, up to 5 cm long omphacite crystals, overgrow syn-D_2 fine-grained omphacite. Syn-D_3 recrystallization of previous amphiboles, phengite and zoisite is observed at their rims. S_4 foliation is marked by fine grained glaucophane and phengite. Shear planes involve 10-cm-thick lens-shaped volumes with the progressive replacement of omphacite and garnet by amphibole. Tension gashes in amphibole-bearing eclogite are filled by medium-grained syntactical growth of clinozoisite, glaucophane and titanite. D_5 is characterized by corona reactions and shear planes and fractures, with the growth of fine-grained albite, chlorite, green amphibole, white mica and epidote.

Zoisite-bearing eclogite

Medium- to fine-grained blue-green amphibole, zoisite and phengite mark the S_1 foliation. Reddish garnet cores preserving inclusions of rutile, blue-green amphibole, zoisite and phengite testify the growth of garnet during the D_1 stage.

Square-shaped pseudomorphs of zoisite and paragonite replace lawsonite. Pseudomorphs are wrapped by S_2 foliation. Kyanite with very fine inclusions of almost pure zoisite, quartz and sodium-calcic amphibole replaces lawsonite, overgrowing S_1 in D_2 low strain domains. Finally, a syn-D_2/D_3 paragonite corona develops around the previous structure (Fig. 5b).

The S_2 foliation is a mm-thick mylonitic foliation, associated with grain size reduction and marked by fine-grained zoisite, phengite, paragonite, glaucophane and omphacite SPO. In syn-D_2 low-strain domains, coarse grained omphacite, phengite and garnet are randomly orientated. In some cases, omphacite and garnet are wrapped by the S_2 foliation (Fig. 5c), in others they cross cut the S_2 foliation. During D_3 amphibole, phengite and zoisite form rims on D_2 assemblages. During D_5 fine-grained albite, chlorite, green amphibole, white mica and epidote develop in pseudomorphs or local millimetre shear zones.

Amphibole-epidote-bearing eclogite

Blue-green amphibole and epidote porphyroclasts represent the only D_1 relics. In syn-D_2 low-strain domains, medium-grained omphacite and phengite with random orientation are found, whereas in high-strain S_2 domains the foliation is marked by fine- to medium-grained blue-green amphibole (Fig. 5d), omphacite, phengite, epidote, chlorite and, locally, pinkish poikiloblastic coarse-grained garnet develop (up to 30%). During D_5, fine-grained albite, chlorite, actinolite, white mica and epidote develop along the S_5 mylonitic foliations and only partially replace previous minerals in low-strain D_5 domains.

Quartz-bearing eclogite

Medium-grained zoisite, phengite and blue-amphibole crystals show a shape preferred orientation SPO and lens shaped quartz domains mark the cm-space discontinuous S_1 foliation. Locally, where S_1 is poorly developed or absent, the syn-D_1 mineral assemblage is recognizable as pseudomorphic replacements of the igneous minerals: calcic plagioclase and primary amphibole are mainly replaced by zoisite and blue amphibole, respectively.

S_2 is a cm-spaced foliation marked by aligned medium-grained zoisite, phengite and omphacite. Coarse-grained and up to 5 cm, randomly oriented, omphacite, phengite and garnet grew in syn-D_2 low-strain domains (Fig. 5e). D_3 is characterized by the recrystallization amphibole, phengite and zoisite.

During D_5 stage large porphyroclasts of amphibole and omphacite are pseudomorphosed by fine-grained albite, chlorite, green amphibole, white mica and epidote aggregates. Omphacite is often boudinaged and boudin necks are filled by albite, chlorite and actinolite. D_5 shear zones are characterized by the growth of fine grained quartz and white mica, with minor chlorite, albite and epidote.

Chlorite-bearing amphibolite

Syn-D_1 relics are represented by pale-green amphibole cores, with exsolutions of white mica along the cleavage planes. The cm-spaced S_2 foliation (Fig. 5f) is marked by amphibole, chlorite, omphacite, epidote and white mica SPO. In D_5 shear planes and fractures fine-grained Fe-chlorite, albite, white mica, medium-grained K-feldspar and epidote occur.

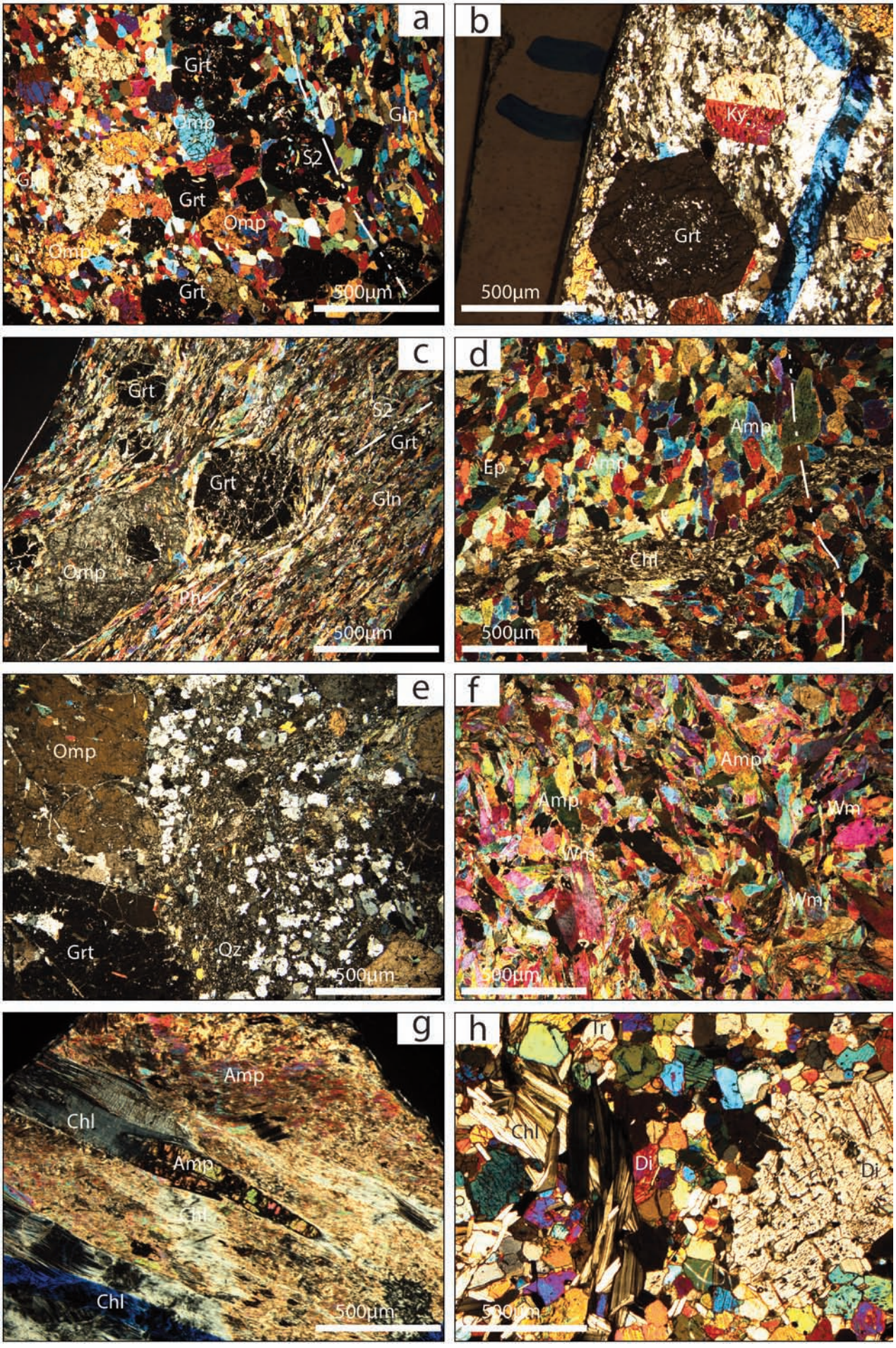
a
Grt
Omp
Gln
S2
Grt
Omp
Omp
Grt
500µm
b
Ky
Grt
500µm
c
Grt
S2
Grt
Grt
Gln
Omp
Ph
500µm
d
Amp
Ep
Amp
Chl
500µm
e
Omp
Grt
Qz
500µm
f
Amp
Amp
Wm
Wm
Wm
500µm
g
Amp
Chl
Amp
Chl
500µm
h
Tr
Chl
Di
Di
500µm

Ultramafites

Antigorite serpentinite: fine-grained antigorite, Mg- chlorite and tremolite mark the mm-sized S_2 foliated fabric. 1- to -10 mm-sized layers of tremolite, diopside and chlorite or antigorite, magnetite and ankerite are locally recognizable as relics in the S_2 foliation (Fig. 5g). Fractures filled by fibrous chrysotile, medium-grained Mg-chlorite and tremolite occur at high angle with the dominant foliation. Hexagonal-shaped textural relics, replaced by antigorite, are probably related to igneous or metamorphic olivine.

Metapyroxenite: fine- to medium-grained isoriented diopside, tremolite (on rims of D_1 amphiboles), phengite, phlogopite and Mg-chlorite mark the S_2 foliation whereas medium- to coarse-grained diopside and tremolite pale cores represent relics of D_1 stage. Medium- to coarse-grained randomly oriented omphacite crystals developed in thinner metapyroxenite layers are rimmed by fine-grained phengite and phlogopite crystals. Mm-thick D_5 shear zones are localized in metapyroxenite. They are associated with the blastesis of fine-grained crystals of Fe-chlorite and albite grown along the S_5 mylonitic foliation.

The deformation-metamorphism relations (Tab. 1) described in the previous sections are coherent to the reconstructions of Zucali et al. (2004), Zucali and Spalla (2011) and Delleani (2013) (Fig. 1c). D_1 occurred at T < 510°C and P < 1.7 GPa. Post-D_1 assemblage (glaucophane, chlorite, phengite, lawsonite, quartz, garnet and zoisite) is stable at T = 510-590°C and P = 1.7-2.05 GPa. The D_2 fabrics, defined by kyanite-bearing eclogite facies conditions assemblage (omphacite, garnet, kyanite), developed at T = 600-620°C and P = 2.2-2.3 GPa, while the retrograde evolution is consistent with T and P decrease during D_3 (T 520-600°C and P = 1.4-1.9 GPa) and D_4 stages (T < 500°C and P < 1.4 GPa), up to D_5 stage (T = 380-520° C and P < 0.8 GPa).

WHOLE ROCK COMPOSITION

The different lithotypes constituting the mafic complex were analyzed to determine whole rock major and trace element composition. One sample for each lithotype was selected from the less deformed domains and, as far as possible, far away from veins and shear zones. Selected samples were analyzed at the ACME lab after lithium borate fusion with ICP-AES for major elements and with ICP-MS for trace elements. Major and trace element composition is reported in Table 2 and Fig. 6.

The two ultramafic lithotypes have a chemical composition significantly different from all the other lithotypes. The *antigorite serpentinite* has low SiO_2 (39.0 wt.%), high MgO (28.4 wt.%) and relatively high Fe_2O_3 (11.7 wt.%). It shows relatively high Ni (1009 ppm) and negligible Na_2O and K_2O contents. The *metapyroxenite* has high SiO_2 (52.0 wt.%), MgO (22.1 wt.%), CaO (13.7 wt.%) and low Al_2O_3 (1.33 wt.%). Significant differences with the serpentinite are observed for Cr (0.38 wt.%) and Ni (115 ppm) contents. The two analyzed ultramafites are the lithotypes with the lowest concentrations in incompatible elements with respect to the other lithotypes. The N-MORB normalized trace element pattern reveals an extreme depletion in heavy rare earth elements (HREE; < 0.1 times N-MORB) and slightly higher concentrations for the LREE (0.2-0.5 times N-MORB). Peculiar of the serpentinite is a positive Sr anomaly relative to the neighboring elements (Fig. 6).

The *quartz-bearing eclogite* and the *zoisite-bearing eclogite* are the lithotypes in the sequence with the highest contents in alkali (Na_2O is up to 3.7 wt.%) and the lowest contents in MgO (down to 7.1 wt.%). Incompatible trace element concentrations are low but slightly higher (HREE are at about 0.2 times N-MORB) than in the ultramafic rocks (Fig. 6). Peculiar of these samples is a marked positive Eu anomaly and a much higher positive anomaly in Sr relative to ultramafic rocks.

Amphibole-epidote-bearing eclogites have generally low SiO_2 contents (38.4-41.8 wt.%) and are characterized by relatively high Al_2O_3 (16.1-21.7 wt.%) and CaO (11.9-19.4 wt.%) contents. Concentrations in incompatible trace elements are the highest among the investigated samples. HREE are at about 1-2 times N-MORB whereas LREE are up to 36 times N-MORB. Both samples show a Nb negative anomaly relative to the neighbouring elements. In these lithotypes high concentrations of Th and U are also observed (up to 216 times N-MORB).

SiO_2 and Al_2O_3 contents in amphibole-bearing eclogite are in the ranges 44.2-48.9 and 9.97-12.95 wt.%, respectively. Fe_2O_3 is up to 17.0 wt.% whereas MgO is in the range 10.1-12.5 wt%. Na_2O and K_2O are below 2.69 and 0.2 wt.%, respectively. The incompatible trace element composition is highly variable. Two amphibole-bearing eclogite samples (G and K) have almost flat REE at about 0.7 times N-MORB. Sample J is much more enriched with concentration for the LREE (3.6 times N-MORB) in between that of the amphibole-epidote bearing eclogite and samples G and K.

The analyzed lithotypes underwent at least Alpine high-pressure equilibration. During high pressure metamorphism element mobility is likely, the bulk rock chemistry is thus expected to partially reflect that of the igneous protolith. The identification of which elements were mobilized during metamorphism is not straightforward. Some elements are well known to be much more immobile than others during metamorphism. If TiO_2 is considered as representative of the more immobile major elements, a relatively good correlation is observed with Al_2O_3 and Fe_2O_3, thus suggesting that for these elements the system was likely closed during the metamorphic evolution. The off-trend behavior of the two ultramafic samples is likely related to their distinct nature

Fig. 5 - Microstructure of rocks from Ivozio mafic complex. a) Amphibole rich layer of the amphibole-bearing eclogite. S_2 is marked by glaucophane, with zoned garnet preserving inclusions of syn-D_1 amphibole at their cores. Garnet rims are inclusion-free and partly overgrow S_2 (crossed polars); b) kyanite crystal with fine-grained inclusion of zoisite and quartz in zoisite-bearing eclogite (crossed polars); c) coarse-grained garnet and omphacite crystals with an internal foliation, gradually oriented parallel to the external mm-spaced S_2 foliation marked by phengite, zoisite, glaucophane and omphacite, in zoisite-bearing eclogite (crossed polars); d) S_2 foliation marked by fine-grained amphibole and epidote, in amphibole-epidote-bearing eclogite (crossed polars); e) large omphacite and garnet crystals close to a quartz-bearing fine-grained domain comprising zoisite and phengite aggregates, in quartz-bearing eclogite (crossed polars); f) mm S_2 foliation mainly marked by medium to fine-grained amphibole with minor white mica and chlorite, in chlorite-bearing amphibolite (crossed polars); g) mm foliation in serpentinite, marked by medium- to fine-grained antigorite, tremolite, white mica and Mg-chlorite (crossed polars); h) diopside relic with numerous inclusion of very fine-grained ilmenite, and rimmed by fine-grained diopside + tremolite granoblastic aggregates in metapyroxenite (crossed polars).

Table 2 - Major and trace element composition of selected lithotypes.

		SiO_2	TiO_2	Al_2O_3	Cr_2O_3	Fe_2O_3	MnO	MgO	CaO	Na_2O	K_2O	P_2O_5	LOI	Sum
		wt.%	wt.%	wt.%	wt.%	wt.%	wt.%	wt.%	wt.%	wt.%	wt.%	wt.%	wt.%	wt.%
A	ultramafites	39.02	0.12	1.68	0.28	11.71	0.18	28.43	5.38	0.02	<0.01	<0.01	12.5	99.32
E	metapyroxenite	52.05	0.07	1.33	0.38	5.76	0.10	22.12	13.67	0.11	<0.01	<0.01	4.0	99.59
B	qtz rich eclogite	46.96	0.22	20.90	0.05	4.34	0.05	7.18	11.91	3.66	0.77	<0.01	3.7	99.74
C	amphibole-epidote-bearing eclogite	38.41	0.63	21.68	0.04	9.27	0.13	4.56	19.43	0.68	0.11	1.30	3.1	99.34
D	amphibole-epidote-bearing eclogite	41.83	0.97	16.16	0.09	10.61	0.15	11.36	12.96	2.09	0.38	0.17	2.8	99.57
F	zoisite bearing eclogite	48.13	0.26	20.34	0.03	5.61	0.08	7.66	11.10	3.31	0.24	<0.01	3.0	99.76
G	amph bearing eclogite	48.86	0.63	12.95	0.05	8.96	0.19	10.10	14.13	2.69	0.03	<0.01	1.1	99.69
J	amph bearing eclogite	47.16	2.27	9.97	0.06	12.24	0.13	12.52	10.94	2.26	0.19	0.07	1.8	99.61
K	amph bearing eclogite	44.19	2.71	12.44	0.03	17.04	0.29	10.08	11.13	1.21	0.05	0.01	0.5	99.68

		Ni	Sc	Zr	Ba	Be	Co	Cs	Ga	Hf	Nb	Rb	Sn	Sr	Ta	Th	U	V	W	Y
		ppm	ppm	ppm	ppm	ppm	ppm	ppm	ppm	ppm	ppm	ppm	ppm	ppm	ppm	ppm	ppm	ppm	ppm	ppm
A	ultramafites	1009	32	3.6	6	<1	109.3	<0.1	4.8	0.1	0.9	0.4	<1	124.1	<0.1	<0.2	<0.1	70	<0.5	2.5
E	metapyroxenite	115	31	3.4	6	<1	46.2	<0.1	3.0	0.1	0.3	0.4	<1	58.0	<0.1	<0.2	<0.1	64	<0.5	2.7
B	qtz rich eclogite	133	22	6.7	376	<1	32.5	2.2	14.4	0.3	0.4	25.5	<1	480.2	<0.1	<0.2	<0.1	160	0.9	5.3
C	amphibole-epidote-bearing eclogite	73	26	75.4	92	<1	17.3	0.3	25.9	1.8	11.3	3.5	22	4010	1.6	21.3	14.1	320	1.4	34.8
D	amphibole-epidote-bearing eclogite	186	40	43.3	189	1	45.2	0.5	15.8	1.0	11.3	6.6	9	1231	0.7	8.8	3.2	334	1.9	20.1
F	zoisite bearing eclogite	112	20	9.0	116	<1	29.8	0.2	13.1	0.4	0.3	5.0	<1	285.5	<0.1	<0.2	<0.1	134	0.7	6.8
G	amph bearing eclogite	49	63	26.1	35	<1	32.5	<0.1	14.0	1.4	0.2	1.0	<1	281.9	<0.1	<0.2	<0.1	404	0.9	21.2
J	amph bearing eclogite	177	47	79.1	23	<1	36.0	<0.1	21.9	2.7	2.3	1.7	<1	262.5	0.2	0.6	0.3	613	1.7	24.5
K	amph bearing eclogite	84	63	37.2	11	<1	62.4	<0.1	15.5	1.7	1.5	0.8	<1	97.4	<0.1	<0.2	0.1	547	1.3	43.5

		La	Ce	Pr	Nd	Sm	Eu	Gd	Tb	Dy	Ho	Er	Tm	Yb	Lu
		ppm	ppm	ppm	ppm	ppm	ppm	ppm	ppm	ppm	ppm	ppm	ppm	ppm	ppm
A	ultramafites	0.9	1.7	0.33	1.7	0.53	0.14	0.60	0.08	0.56	0.12	0.25	0.04	0.23	0.03
E	metapyroxenite	1.5	4.0	0.69	3.6	0.79	0.18	0.74	0.09	0.58	0.10	0.24	0.04	0.22	0.04
B	qtz rich eclogite	1.6	2.4	0.38	2.0	0.64	0.59	0.87	0.14	1.05	0.19	0.53	0.08	0.51	0.07
C	amphibole-epidote-bearing eclogite	117.6	247.1	28.55	111.2	16.56	4.75	12.21	1.24	7.30	1.18	2.94	0.41	2.60	0.36
D	amphibole-epidote-bearing eclogite	46.6	100.7	11.99	47.9	8.10	2.23	6.03	0.70	4.04	0.66	1.80	0.24	1.42	0.23
F	zoisite bearing eclogite	1.8	2.9	0.43	2.5	0.72	0.62	1.03	0.16	1.01	0.22	0.58	0.08	0.58	0.07
G	amph bearing eclogite	2.3	5.7	1.10	6.1	2.39	0.77	3.36	0.56	4.05	0.73	2.28	0.34	2.35	0.31
J	amph bearing eclogite	11.8	31.6	5.31	29.5	10.64	3.61	9.91	0.94	4.74	0.91	2.52	0.39	2.83	0.41
K	amph bearing eclogite	2.1	5.3	0.93	5.4	2.36	0.91	5.18	1.02	8.00	1.56	4.83	0.64	3.85	0.59

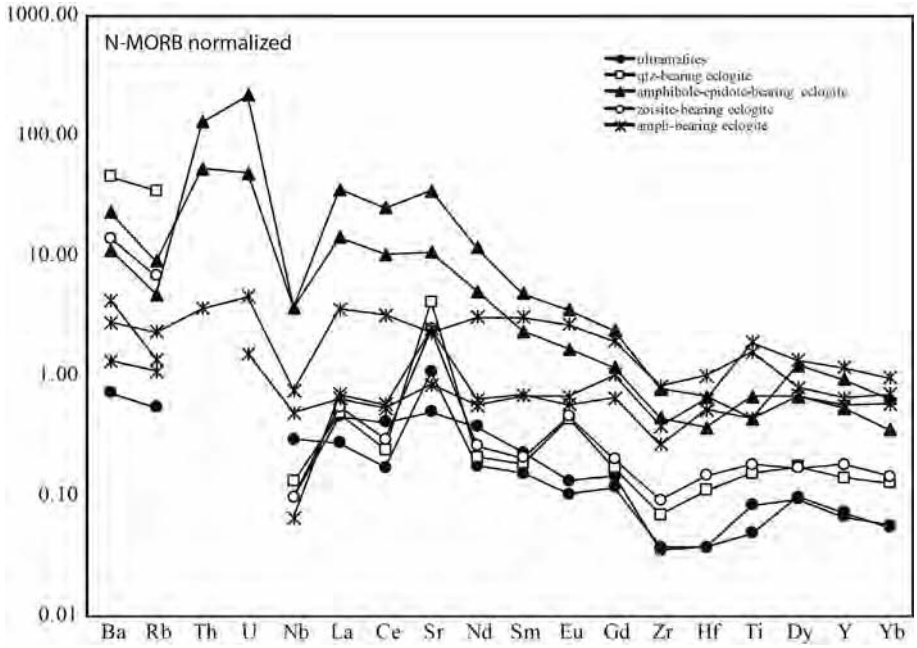

Fig. 6 - N-MORB normalized incompatible element diagram for the different litotypes constituting the Ivozio mafic complex.

(mantle/cumulus) relative to the other lithotypes. A general poor correlation is observed between TiO_2, CaO and the alkalis, thus suggesting that these last elements were mobile during metamorphism. Zr is considered, among trace elements, one of the most immobile elements and it shows good correlation with other immobile elements such as Y, HREE and V. This confirms that for these elements the system was likely closed during metamorphism. Nb, which is considered an immobile element and that has a similar incompatible behaviour do not correlate with Zr. This unexpected result may suggest that all the rocks of the Ivozio mafic complex may be not necessarily cogenetic, otherwise Nb has been selectively mobilized. Correlation of Zr with large ion lithophile elements (LILE) is poor in agreement with the high mobility of the latter elements.

DISCUSSION AND CONCLUSIONS

The structural and metamorphic Alpine evolution (Zucali and Spalla, 2011; Delleani et al., 2012b; Delleani, 2013) suggests that the burial and exhumation of the Ivozio mafic complex (D_1-D_4 interval) is characterized by a thermal gradient ≤ 10°C/km, compatible with a cold active oceanic subduction. This agrees with the evolution of other portions of SLZ (e.g., Roda et al., 2012). Moreover, peak conditions reached during D_2 are accomplished after a prograde P-T path in the lawsonite-stability field. This prograde P-T path is characterized by a P/T ratio typical of cold subduction zones (e.g., Cloos, 1993). This P/T ratio persists up to the PT-peak conditions, achieved at the beginning of D_2. The subsequent P retrograde evolution is associated to P/T ratios higher than that of prograde evolution. Such retrograde conditions are comprised between those of warm subduction zones and of plate interiors (e.g., Cloos, 1993). Only the last exhumation stage occurred under PT conditions compatible with continental collision. Mechanical and chemical re-equilibrations recorded under eclogite-facies conditions occurred at 65±3 Ma according to U/Pb determinations on zircons of Montestrutto metapelites (Rubatto et al., 1999), which are part of the gabbroic Complex country rocks. Considering the polyphase structural evolution, occurred under eclogite-facies conditions, it is for now impossible to relate such age to late-D_1, D_2 or D_3 re-equilibration - deformation stages. In addition, the only available U/Pb ages from Ivozio eclogites range between 79 and 70 Ma and have been inferred from less than 10 mm bright zircon rims (Rubatto, 1998).

The preservation of a wide portion of the prograde and peak metamorphic history of the Ivozio mafic complex was possible thank to the km-scale strain partitioning between strong metagabbros and surrounding weaker micaschists and gneisses. This also allowed the partial reconstruction of the pre-Alpine igneous lithostratigraphy (Fig. MAP). In the less deformed domains, where strain partitioning allows the preservation of pristine igneous zoning, it was recognized a possible magmatic layering marked by alternating amphibole-bearing and zoisite-bearing eclogite and quartz-bearing eclogite layers representing a cumulitic sequence from gabbro to leucogabbro. In the described lithologic assemblage, meta-pyroxenite and antigorite-serpentinite layers can be derived from both mantle enclaves or from ultramafic cumulus rocks.

Most of the lithotypes show a negative Nb anomaly, which is typical of subduction related melts. However, because La is a relatively mobile element the significance of the Nb/La ratio for geodynamic interpretations can be questioned. Furthermore, low Nb/La ratios are typical of the continental crust. The Ivozio mafic complex is enclosed into the continental crust and in turn crustal contamination may have increased the Nb negative anomaly simulating a subduction related geological setting. The generally very low concentrations of immobile incompatible trace elements (e.g., Zr, Y and HREE) in the quartz-bearing eclogites and in the zoisite-bearing eclogites may suggest an origin of the parental liquid from highly refractory mantle sources that experienced previous partial melting events such as in an arc or back-arc setting. Notwithstanding, we cannot exclude that during metamorphism the rocks suffered a significant depletion in trace elements that affected also the more immobile elements.

Although the geochemical signature of the Ivozio mafic complex could be compatible with an origin in a subduction environment, whole rock geochemistry alone cannot clearly assign the studied rocks to a particular geodynamic setting. In fact, any robust geodynamic inference on the basis of the geochemical data of the Ivozio samples is hampered by two limitations: i) little is known about how much metamorphism has promoted element mobility in the studied rocks; ii) little or no constraints about how much the bulk rock chemistry can reflect that of the parental liquid.

The first question is solved by detailed meso- and microstructural strain analysis, which permitted to precisely select domains where the Alpine mechanical and metamorphic re-equilibration was low enough to reconstruct the original lithological differentiation, suggesting that at least the highly immobile elements were not redistributed during metamorphism. Based on this constraint we can distinguish two main rock types within the Ivozio mafic complex magmatic suite:

- type I - highly depleted rocks (ultramafic rocks, quartz-bearing eclogites and zoisite bearing eclogites);
- type II - variably enriched rocks (amphibole-epidote bearing eclogites and amphibole bearing eclogites).

Type I rocks have discriminative elements such as Ta, Yb and Th below the detection limits, thus only type II rocks can be classified using this approach. Under the hypothesis that the composition of the studied rocks resembles that of a melt, in the Th/Ta vs. Yb discrimination diagram (Gorton and Shandl, 2000) two type II rocks plot in the field of active continental margin (subduction related) and one in the field of within plate volcanics (Fig. 7). The geodynamic affinity of the type I samples is difficult to address. The very low concentrations in immobile incompatible trace elements (e.g., Nb and Yb) suggests an origin from a depleted to highly refractory mantle source. The Nb/Yb ratios are very close to those of MORB and absolute element concentrations are close to those of boninites (e.g., Kelemen et al., 2003). Highly immobile elements in type I rocks thus may still suggest a supra-subduction origin (Fig. 7). In addition, the Ti-V and TiO_2-MgO contents of Ivozio mafic and ultramafic rocks are compatible with the compositions of subduction-related magmatic series according to Dilek and Furnes (2011), thus further supporting this idea.

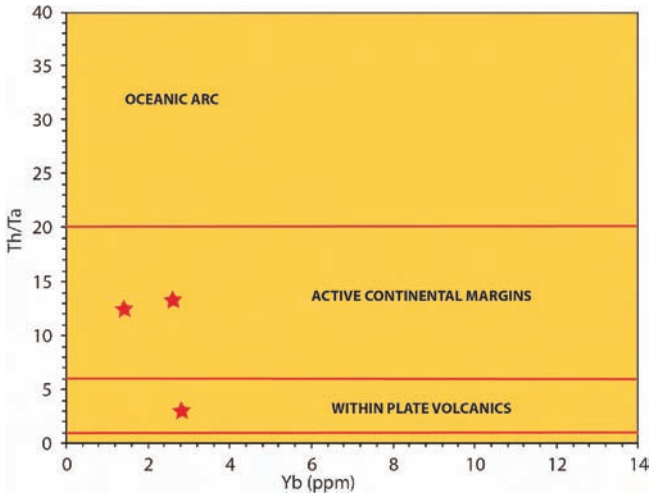

Fig. 7 - Th/Ta vs Y diagram for studied Ivozio mafic complex.

In conclusion, the whole rock major and trace element compositions, obtained sampling the less deformed domains, and excluding volumes close to veins and shear zones, suggest that all the Ivozio igneous rocks may be not co-genetic and that they probably emplaced in the continental crust in a subduction-related context.

Taking into account that the continental crust surrounding the Ivozio mafic complex is pre-Alpine, it is useful to check the occurrence of corresponding subduction-related igneous products, or lithostratigraphic associations, in the European Variscan crust of Late Devonian to Early Carboniferous age. Actually, igneous products and sedimentary sequences interpreted as characteristic of volcanic arc and back-arc geodynamic settings occur in different portions of French Central Massif, Vosges and Bohemian Massif with ages spanning from 385 to 345 Ma (Lardeaux et al. 2014 and references therein) (Fig. 8). The Ivozio mafic complex protoliths can therefore be interpreted as witnesses of such Devonian-Carboniferous arc/back-arc setting in the Alpine chain. The occurrence of subduction-related garnet-bearing

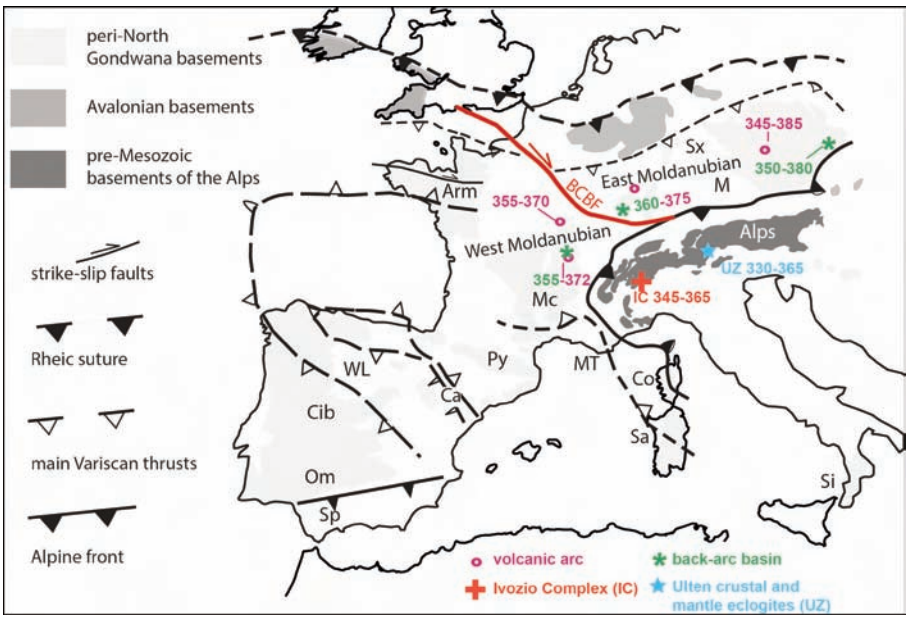

Fig. 8 - Simplified tectonic sketch (modified after Spalla et al. 2014 and references therein) of the European Variscides with the location and ages of volcanic arc and back-arc basin rocks of Devonian-Carboniferous age according to Lardeaux et al. (2014). Ivozio mafic complex (IC) and Ulten eclogites (UZ) are also located. Arm- Armorica; Ca- Cantabrian terrane; Cib- Central Iberian; Co- Corsica; M- Moldanubian Units; MC- French Central Massif; MT- Maures-Tanneron Massif; OM- Ossa Morena; Py- Pyrenees; Sa- Sardinia; Si- Sicilian-Apulian basements; SP- South Portuguese Zone; Sx- Saxothuringia; WL- West Asturian-Leonese; BCBF- Bristol Channel-Bray Fault (after Edel et al., 2013; Lardeaux et al., 2014).

peridotites and eclogites of the Ulten Complex (Austroalpine domain of Eastern Alps; 330-365 Ma; Godard et al., 1996; Tumiati et al., 2003; 2007) reinforces this conclusion. The Ivozio mafic complex, with its surrounding continental rocks, can represent the arc remnants contemporaneous with the Ulten Late Devonian-Early Carboniferous subduction complex, in a Variscan geodynamic setting.

The spatial distribution from the French Massif Central to the Bohemian Massif of Late Devonian-Early Carboniferous igneous and sedimentary products indicating back-arc and volcanic arc settings, respectively, suggested to envisage a South- to South-East-dipping subduction zone, active during this time interval (e.g., Edel and Schulmann, 2009; Edel et al., 2013; Lardeaux et al., 2014 and references therein). In the case of the French Massif Central magmatic arc-related rocks are volcanic and sedimentary. On the contrary, in the Bohemian Massif, they are dominated by calc-alkaline mainly intermediate intrusive rocks, associated with minor acidic and more basic types, including gabbros, similarly to what occurs in the Ivozio mafic complex. The shallowest crustal rocks crop out in the portion of the Variscan belt West of the Bristol Channel-Bray Fault (BCBF Fig. 8). This supports the interpretation envisaging that the sector West of the BCBF (West Moldanubian Zone) represents a more superficial structural level of the Late Devonian-Early Carboniferous crust with respect to the sector surfacing East of the Fault, the East Moldanubian Zone (Lardeaux et al., 2014 and references therein). In this light, the crust enclosing the Ivozio mafic complex may be interpreted as of eastern Moldanubian affinity, even if located at present West of the BCBF. BCBF does not extend to the Alpine region because it is truncated toward the South by the Alpine Front (Fig. 8): the strong tectonic reworking recorded by the Ivozio mafic complex during Alpine subduction and collision imposes serious caution on any possible paleogeographic restoration.

ACKNOWLEDGEMENTS

G. Capponi and an anonymous reviewer are thanked for their critical reading. F.D., G.R., M.Z. and M.I.S. acknowledge funding from MIUR (Ministero dell'Istruzione, dell'Università e della Ricerca) PRIN 2010-2011 (grant number 2010AZR98L) 'Birth and death of oceanic basins: geodynamic processes from rifting to continental collision in Mediterranean and circum-Mediterranean orogens'. A. Giovanetto is thanked for his logistic support and inspiring fluid-supply. The supplementary material (cited in the text as Fig. MAP) is available at the web address www.ofioliti.it

REFERENCES

Babist J., Handy M.R., Konrad-Schmolke M. and Hammerschmidt K., 2006. Precollisional, multistage exhumation of subducted continental crust: The Sesia Zone, western Alps. Tectonics, 25, TC6008, doi:10.1029/2005TC001927

Bertotti G. and der Voorde M., 1994. Thermal effects of normal faulting during rifted basin formation, 2. The Lugano-Valgrande normal fault and the role of pre-existing thermal anomalies. Tectonophysics, 240: 145-157, doi: 10.1016/0040-1951 (94)90269-0;

Bertotti G., Picotti V., Bernoulli D. and Castellarin A., 1993. From rifting to drifting: tectonic evolution of the South-Alpine Late crust from the Triassic to the Early Cretaceous. Sedim. Geol., 86: 53-76.

Bianchi A., Dal Piaz G.B. and Viterbo C., 1965. Le masse di anfiboliti gabbriche a gastaldite di Corio e Monastero e di alter località della Zona Sesia-Lanzo (Alpi Occidentali). Mem. Accad. Sci. Torino, 4: 1-36.

Bigi G., Castellarin A., Coli M., Dal Piaz G.V., Sartori R., Scandone P. and Vai G.B., 1990. Structural Model of Italy, sheets 1-2, In: C.N.R., P.F.G. (Ed.). S.E.L.C.A., Florence.

Bussy F., Venturini C., Hunziker J. and Martinotti G., 1998. U-Pb ages of magmatic rocks of the Western Austroalpine Dent Blanche-Sesia Unit. Schweiz. Miner. Petrogr. Mitt., 78: 163-168.

Cantù M., Spaggiari L., Zucali M., Zanoni D. and Spalla M.I., 2016. Structural analysis of a subduction- related contact in southern Sesia-Lanzo Zone (Austroalpine Domain, Italian Western Alps). J. Maps: 22-35, doi: 10.1080/17445647.2016.

Castelli D., 1991. Eclogitic metamorphism in carbonate rocks: the example of impure marbles from the Sesia-Lanzo Zone, Italian Western Alps. J. Metam. Geol., 9: 61-77.

Cenki-Tok B., Oliot E., Rubatto D., Berger A., Engi M., Janots E., Thomsen T.B., Manzotti P., Regis D., Spandler C., Robyr M. and Goncalves P., 2011. Preservation of Permian allanite within an Alpine eclogite facies shear zone at Mt. Mucrone, Italy: Mechanical and chemical behavior of allanite during mylonitization. Lithos, 125: 40-50.

Cloos M., 1993. Lithospheric buoyancy and collisional orogenesis - Subduction of oceanic plateaus, continental margins, island arcs, spreading ridges, and seamounts. Geol. Soc. Am. Bull., 105: 715-737.

Compagnoni R., Dal Piaz G.V., Hunziker J.C., Gosso G., Lombardo B. and Williams P.F., 1977. The Sesia-Lanzo Zone, a slice of continental crust with Alpine high pressure-low temperature assemblages in the Western Italian Alps. Rend. S.I.M.P., 33: 281-334.

Corti L., Alberelli G., Zanoni D. and Zucali M., 2017. Analysis of fabric evolution and metamorphic reaction progress at Lago della Vecchia-Valle d'Irogna, Sesia-Lanzo Zone, Western Alps. J. Maps, 13 (2): 521-533.

Dal Piaz G. V., Gosso G. and Martinotti G., 1971. La II Zona Diorito-kinzigitica tra la Valsesia e la Valle d'Ayas (Alpi Occidentali). Mem. Soc. Geol. It., 10: 257-276.

Dal Piaz G.V., 1993. Evolution of Austro-Alpine and Late Penninic basement in the northwestern Alps from Variscan convergence to post-Variscan extension. In: J. Von Raumer and F. Neubauer (Eds.), Pre-Mesozoic geology in the Alps. Springer-Verlag, Berlin, p. 327- 344.

Dal Piaz G.V., Hunziker J.C. and Martinotti G., 1972. La Zona Sesia-Lanzo e l'evoluzione tettonico-metamorfica delle Alpi Nordoccidentali interne. Mem. Soc. Geol. It., 11: 433-460.

Delleani F., 2013. Deformation and metamorphism relationships in acid and mafic protoliths of the Austroalpine continental crust subducted and exhumed in a severely depressed thermal regime. PhD thesis, Univ. Studi Milano, 152 pp.

Delleani F., Spalla M.I., Castelli D. and Gosso G., 2012a. Multiscale structural analysis in the subducted continental crust of the internal Sesia-Lanzo Zone (Monte Mucrone, Western Alps). J. Virt. Expl., 41, paper 7, doi: 10.3809/jvirtex.2011.00287

Delleani F., Spalla M.I., Castelli D. and Zucali M., 2011. Structural mapping of a Lower Carboniferous gabbro eclogitised during Alpine convergence (Sesia-Lanzo Zone,Western Alps). Rend. online S.G.I., 15: 56-59.

Delleani F., Spalla M.I., Rebay G. and Zucali M., 2012b. Tectonometamorphic evolution of the Ivozio Complex (Sesia-Lanzo, Western Alps). Rend. online S.G.I., 22: 69-72.

Diella V., Spalla M.I. and Tunesi A., 1992. Contrasting thermomechanical evolutions in the South-Alpine metamorphic basement of the Orobic Alps (Central Alps, Italy). J. Metam. Geol., 10: 203-219.

Dilek Y. and Furnes H., 2011. Ophiolite genesis and global tectonics: Geochemical and tectonic fingerprinting of ancient oceanic lithosphere. Geol. Soc. Am. Bull., 123 (3/4): 387-411, doi: 10.1130/B30446.1

Edel J. B. and Schulmann K., 2009. Geophysical constraints and model of the 'Saxothuringian and Rhenohercynian subductions - magmatic arc system' in NE France and SW Germany. Bull. Soc. Géol. Fr., 180: 545-558.

Edel J.B., Schulmann K., Skrzypek E. and Cocherie A., 2013. Tectonic evolution of the European Variscan belt constrained by palaeomagnetic, structural and anisotropy of magnetic susceptibility data from the Rhenohercynian magmatic arc (Northern Vosges, Eastern France). J. Geol. Soc. London, 170: 785-804.

Godard G., Martin S., Prosser G., Kienast J.R. and Morten L., 1996. Variscan migmatites, eclogites and garnet-peridotites of the Ulten Zone, Eastern Austroalpine system. Tectonophysics, 259: 313-341, doi:10.1016/0040-1951(95)00145-X

Gorton M.P. and Schandl E.S. 2000. From continents to island arcs: a geochemical index of tectonic setting for arc-related and within-plate felsic to intermediate volcanic rocks. Can. Miner., 38: 1065-1073.

Gosso G., 1977. Metamorphic evolution and fold history in the eclogite micaschists of the Late Gressoney Valley (Sesia-Lanzo Zone, Western Alps). Rend. S.I.M.P., 33: 389-407.

Gosso G., Messiga B., Rebay G. and Spalla M.I., 2010. Amphibolite eclogitisation in Sesia-Lanzo Zone (Western Alps): deformation and rock chemistry as controllers of metamorphic reactions. Int. Geol. Rev., 52: 1193-1219.

Gosso G., Rebay G., Roda M., Spalla M.I., Tarallo M., Zanoni D. and Zucali M., 2015. Taking advantage of petrostructural heterogeneities in subduction-collisional orogens, and effect on the scale of analysis. Per. Miner., 84: 779-825.

Handy M.R. and Oberhänsli R., 2004. Metamorphic structure of the Alps; explanatory notes to the map 1:100000. Mitt. Oester. Miner. Ges. Print., 149: 201-226.

Handy M.R., Franz L., Heller F., Janott B. and Zurbriggen R., 1999. Multistage accretion and exhumation of the continental crust (Ivrea crustal section, Italy and Switzerland). Tectonics, 18 (6): 1154-1177, doi: 10.1029/1999TC900034

Hunziker J.C., 1974. Rb-Sr and K-Ar age determinations and the Alpine tectonic history of the Western Alps. Mem. Ist. Geol. Miner. Univ. Padova, 31, 54 pp.

Hunziker J.C., Desmons J. and Hurford A.J., 1992. Thirty-two years of geochronological work in the Central and Western Alps: a review on seven maps. Mém. Géol. Lausanne, 13: 1- 59.

Kelemen P.B., Hanghøj K. and Greene A.R., 2003. One view of the geochemistry of subduction-related magmatic arcs, with an emphasis on primitive andesite and lower crust. In: R.L. Rudnick, H.D. Holland and K.K. Turekian (Eds.), Treatise on Geochemistry, Volume 3, Elsevier, p. 593-659.

Koons P.O., 1982. An investigation of experimental and natural high-pressure assemblages from Sesia Zone, Western Alps, Italy. PhD Thesis, ETH Zürich, 261 pp.

Lardeaux J.M., 1981. Evolution tectono-metamorphique de la zone nord du Massif de Sesia- Lanzo (Alpes occidentales): un exemple d'éclogitisation de croute continentale. PhD Thesis, Univ. Paris VI, 226 pp.

Lardeaux J.M. and Spalla M.I., 1991. From granulites to eclogites in the Sesia Zone (Italian Western Alps): a record of the opening and closure of the Piedmont ocean. J. Metam. Geol., 9: 35-59.

Lardeaux J.M., Gosso G., Kienast J.R. and Lombardo B., 1982. Relations entre le métamorphisme et la déformation dans la zone Sésia-Lanzo (Alpes Occidentales) et le problème de l'éclogitisation de la croûte continentale. Bull. Soc. Géol. Fr., 24: 793-800.

Lardeaux J.M., Schulmann K., Faure M., Janoušek V., Lexa O., Skrzypek E., Edel J.B. and Štípská P., 2014. The Moldanubian Zone in the French Massif Central, Vosges/Schwarzwald and Bohemian Massif revisited: differences and similarities. In: K. Schulmann, J.R. Martínez Catalán, J.M. Lardeaux, V. Janoušek and G. Oggiano (Eds.), The Variscan Orogeny: Extent, Timescale and the Formation of the European Crust. Geological Society London, Special Publications, 405: p. 7-44, doi: 10.1144/SP405.15.

Manzotti P. and Zucali M., 2013. The pre-Alpine tectonic history of the Austroalpine continental basement in the Valpelline unit (Western Italian Alps). Geol. Mag., 150 (1): 153-172, doi: 10.1017/s0016756812000441.

Marotta A.M., Roda M., Conte K. and Spalla M.I., 2016. Thermomechanical numerical model of the transition from continental rifting to oceanic spreading: the case study of the Alpine Tethys. Geol. Mag., in press: 1-30, doi:10.1017/S0016756816000856

Marotta A.M., Spalla M.I. and Gosso G., 2009. Upper and lower crustal evolution during lithospheric extension: numerical modelling and natural footprints from the European Alps. In: U. Ring and B. Wernicke (Eds.), Extending a continent: Architecture, rheology and heat budget. Geol. Soc. London Spec. Publ., 321: 33-72, doi: 10.1144/SP321.3.

Oberhänsli R., Hunziker J.C., Martinotti G. and Stern W.B., 1985. Geochemistry, geochronology and petrology of Monte Mucrone: an example of Eo-Alpine eclogitization of Permian Granitoids in the Sesia-Lanzo Zone, Western Alps, Italy. Chem. Geol., 52: 165-184.

Pognante U., 1989a. Lawsonite, blueschist and eclogite formation in the southern Sesia Zone (Western Alps, Italy). Eur. J. Miner., 1: 89-104.

Pognante U., 1989b. Tectonic implications of lawsonite formation in the Sesia Zone (Western Alps). Tectonophysics, 162: 219-227.

Pognante U., Compagnoni R. and Gosso G., 1980. Micro-mesostructural relationships in the continental eclogitic rocks of the Sesia-Lanzo Zone: a record of a subduction cycle (Italian Western Alps). Rend. S.I.M.P., 36: 169-186.

Rebay G. and Messiga B., 2007. Prograde metamorphic evolution and development of chloritoid bearing eclogitic assemblages in subcontinental metagabbro (Sesia-Lanzo Zone, Italy). Lithos, 98: 275-291.

Rebay G. and Spalla M.I., 2001. Emplacement at granulite facies conditions of the Sesia-Lanzo metagabbros: an early record of Permian rifting? Lithos, 58: 85-104.

Rebay G., Riccardi M.P. and Spalla M.I., 2015. Fluid rock interactions as recorded by Cl-rich amphiboles from continental and oceanic crust of italian orogenic belts. Per. Miner., 84 (3B): 751-777, doi: 10.2451/2015PM0453.

Reddy S.M., Kelley S.P. and Wheeler J., 1996. A $^{40}Ar/^{39}Ar$ laser probe study of micas from the Sesia Zone, Italian Alps: implications for metamorphic and deformation histories. J. Metam. Geol., 14: 493-508.

Regis D., Rubatto D., Darling J., Cenki-Tok B., Zucali M. and Engi M., 2014. Multiple metamorphic stages within an eclogite-facies terrane (Sesia Zone, Western Alps) revealed by Th-U-Pb petrochronology. J. Petrol., 55: 1429-1456, doi: 10.1093/petrology/egu029

Reinsch D., 1979. Glaucophanites and eclogites from Val Chiusella, Sesia-Lanzo Zone (Italian Alps). Contrib. Miner. Petrol., 70: 257-266.

Roda M., Spalla M.I. and Marotta A.M., 2012. Integration of natural data within a numerical model of ablative subduction: a possible interpretation for the Alpine dynamics of the Austroalpine crust. J. Metam. Geol., 30: 973-996.

Rubatto D., 1998. Dating of pre-Alpine magmatism, Jurassic ophiolites and Alpine subductions in the Western Alps. PhD thesis Swiss Federal Inst. Techn. Zurich, 174 pp.

Rubatto D., Gebauer D. and Compagnoni R., 1999. Dating of eclogite-facies zircons; the age of Alpine metamorphism in the Sesia-Lanzo Zone (Western Alps). Earth Planet. Sci. Lett., 167: 141-158.

Rubatto D., Regis D., Hermann J., Boston K., Engi M., Beltrando M. and McAlpine S.R.B., 2011. Yo-yo subduction recorded by accessory minerals in the Italian Western Alps. Nature Geosci., 4: 338-342, doi: 10.1038/ngeo1124.

Schuster R. and Stuewe K., 2008. Permian metamorphic event in the Alps. Geology, 36 (8): 603-606, doi: 10.1130/G24703A.1

Schuster R., Scharbert S., Abart R. and Frank W., 2001. Permo-Triassic extension and related HT/LP metamorphism in the Austroalpine-Southalpine realm. Mitt. Ges. Geol. Bergb. Oester., 45: 111-141.

Spalla M.I. and Marotta A.M., 2007. P-T evolutions vs. numerical modeling: a key to unravel the Paleozoic to Early-Mesozoic tectonic evolution of the Alpine area. Per. Miner., 76: 267-308.

Spalla M.I. and Zulbati F., 2003. Structural and petrographic map of the southern Sesia-Lanzo Zone (Monte Soglio - Rocca Canavese, Western Alps, Italy). Mem. Sci. Geol. Padova, 55: 119-127.

Spalla M.I., De Maria L., Gosso G., Miletto M. and Pognante U. 1983. Deformazione e metamorfismo della Zona Sesia-Lanzo meridionale al contatto con la falda piemontese e con il massiccio di Lanzo, Alpi Occidentali. Mem. Soc. Geol. It., 26: 499-514.

Spalla M.I., Gosso G., Marotta A.M., Zucali M. and Salvi F., 2010. Analysis of natural tectonic systems coupled with numerical modelling of the polycyclic continental lithosphere of the Alps. Intern. Geol. Rev., 52: 1268-1302.

Spalla M.I., Lardeaux J.M., Dal Piaz G.V. and Gosso G., 1991. Metamorphisme et tectonique a la marge externe de la zone Sesia-Lanzo (Alpes occidentales). Mem. Sci. Geol. Padova, 43: 361-369.

Spalla M.I., Zanoni D., Marotta A.M., Rebay G., Roda M., Zucali. M. and Gosso G., 2014. The transition from Variscan collision to continental break-up in the Alps: insights from the comparison between natural data and numerical model predictions. In: K. Schulmann, J.R. Martínez Catalán, J.M. Lardeaux, V. Janoušek and G. Oggiano (Eds.), The Variscan Orogeny: Extent, timescale and the formation of the European crust. Geol. Soc. London Spec. Publ., 405: 363-400, doi: 10.1144/SP405.15.

Stoeckhert B., Jaeger E. and Voll G., 1986. K-Ar age determinations on phengites from the internal part of the Sesia Zone, lower Aosta Valley (Western Alps, Italy). Contrib. Miner. Petrol., 92: 456-470, doi: 10.1007/BF00374428

Stuenitz H., 1989. Partitioning of metamorphism and deformation in the boundary region of the "Seconda Zona Diorito-Kinzigitica", Sesia Zone, Western Alps (Unpubl. PhD thesis). ETH, Zurich, 244 pp.

Tropper P. and Essene E.J., 2002. Thermobarometry in eclogites with multiple stages of mineral growth: an example from the Sesia-Lanzo Zone (Western Alps, Italy). Schweiz. Miner. Petrogr. Mitt., 82: 487-514.

Tropper P., Essene E.J., Sharp Z.D. and Hunziker J.C., 1999. Application of K-feldsparjadeite- quartz barometry to eclogite facies metagranites and metapelites in the Sesia Lanzo Zone (Western Alps, Italy). J. Metam. Geol., 17 (2): 195-209.

Tumiati S., Godard G., Martin S., Klötzli U. and Monticelli D., 2007. Fluid-controlled crustal metasomatism within a high-pressure subducted mélange (Mt. Hochwart, Eastern Italian Alps). Lithos, 94: 148-167.

Tumiati S., Thoni M., Nimis P., Martin S. and Mair V., 2003. Mantle-crust interactions during Variscan subduction in the Eastern Alps (Nonsberg-Ulten Zone): geochronology and new petrological constraints. E.P.S.L., 210: 509-526, doi:10.1016/S0012-821X(03)00161-4

Venturini G., 1995. Geology, geochemistry and geochronology of the inner central Sesia Zone (Western Alps - Italy). Mém. Géol. Lausanne, 25: 1-148.

Venturini G., Hunziker J.C. and Pfeiffer H.R., 1996. Geochemistry of mafic rocks in the Sesia Zone (Western Alps): new data and interpretations. Ecl. Geol. Helv., 89: 369-388.

Venturini G., Martinotti G. and Hunziker J.C., 1991. The protoliths of the "Eclogitic Micaschists" in the lower Aosta Valley (Sesia-Lanzo Zone, Western Alps). Mem. Sci. Geol., 43: 347-359.

Viterbo-Bassani C. and Blackburn C., 1968. The eclogitic rocks of the 'Eclogitic Micaschist Formation', Sesia-Lanzo Zone (Western Alps, Italy). Mem. Sci. Geol. Padova, 27: 1-45.

Wheeler J., and Butler R.W.H., 1993. Evidence for extension in the western Alpine orogen: The contact between the oceanic Piemonte and overlying continental Sesia units. E.P.S.L., 117: 457-474, doi: 10.1016/0012-821X(93)90097-S

Whitney D.L. and Evans B.W., 2010, Abbreviations for names of rock-forming minerals. Am. Miner., 95: 185-187, doi: 10.2138/am.2010.3371.

Williams P.F. and Compagnoni R., 1983. Deformation and metamorphism in the Bard area of the Sesia-Lanzo Zone, Western Alps, during subductionand uplift. J. Metam. Geol., 1: 117-140.

Zucali M., 2011. Coronitic microstructures in patchy eclogitised continental crust: The Lago della Vecchia pre-Alpine metagranite (Sesia-Lanzo Zone, Western Italian Alps). J. Virt. Expl., 38.

Zucali M. and Spalla M.I., 2011. Prograde lawsonite in continental crust: the low-T record of rock flow during the Alpine subduction. J. Struct. Geol., 33: 381-398.

Zucali M., Spalla M.I. and Gosso G., 2002. Fabric evolution and reaction rate as correlation tool: the example of the Eclogitic Micaschists Complex in the Sesia-Lanzo Zone (Monte Mucrone - Monte Mars, Western Alps Italy). Schweiz. Miner. Petrogr. Mitt., 82: 429-454.

Zucali M., Spalla M.I., Gosso G., Racchetti S. and Zulbati F., 2004. Prograde LWS-KY transition during subduction of the Alpine continental crust of the Sesia-Lanzo Zone: the Ivozio Complex. In: M. Beltrando, G. Lister, J. Ganne, and A. Boullier (Eds.), Evolution of the Western Alps: Insights from metamorphism, structural geology, tectonics and geochronology. Eds. J. Virt. Expl., 16 (4): 1-21.

Received, July 9, 2017
Accepted, December 21, 2017